Polymer Vol. 39 No. 19, pp. 4461–4487, 1998

0032-3861/98/$19.00+0.00

PII: S0032-3861(97)10320-2

polymer papers

The role of metastability in polymer phase transitions

Andrew Keller[a,*] and Stephen Z. D. Cheng[b]
[a]*H. H. Wills Physics Laboratory, The University of Bristol, Bristol BS8 1TL, UK*
[b]*The Maurice Morton Institute and Department of Polymer Science, The University of Akron, Akron, OH 44325-3909, USA*
(Received 3 August 1997; revised 8 November 1997)

Polymer phases can be described in the same way as phases in other condensed matter using a number density operator and its correlation functions. This description requires the understanding of both symmetry operations and order at different atomic and molecular levels. Statistical mechanics provides a link between the microscopic description of structure and motion and the macroscopic thermodynamic properties. Within the limits of the laws of thermodynamics, polymers exhibit a rich variety of phase transition behaviours. By definition, a first-order phase transition in a temperature–pressure ensemble describes a transformation which involves a discontinuous change of all the thermodynamic functions but the Gibbs free energy at the transition temperature. Higher-ordered phase transitions are classified as critical phenomena. Of special interest is the role of metastability in phase and phase transition behaviours. A classical metastable state possesses a local free energy minimum, but it is not at the global stable equilibrium. Further, the existence of circumstantial metastability need to be invoked based on the constraints of size, dimensionality, order and symmetry; examples include polymorphism, mesophase concepts, crystal size, and thin film effects. Metastable behaviour is also observed in phase transformations that are impeded by kinetic limitations along the pathway to thermodynamic equilibrium. This is illustrated in structural and morphological investigations of crystallization and mesophase transitions, liquid–liquid phase separation, vitrification and gel formation, as well as combinations of all such transformation processes. In these cases, the metastable state often becomes the dominant state for the entire system, and is observed over a range of time and size scales. This review will describe the general principles of metastability in polymer phases and phase transitions and will provide illustrations from current experimental works in selected areas together with raising so far unaddressed conceptual issues of wider applicability to phase transformations in general.

(Keywords: metastable state; metastability; polymer)

PHASES AND PHASE TRANSITIONS

States of matter and *transformations* between these states are the subject of condensed matter physics. It is well known that solids, liquids, and gases are the three basic states of matter. From a microscopic point of view, arbitrary translation, rotation, and reflection are described by the *Euclidean* group. Since a fluid (liquid or gas) is invariant under all of these operations, its symmetry group is the Euclidean group. Fluids have the highest possible symmetry. Namely, they have the largest number of symmetry operations. This implies that fluids have short-range order but no long-range order. Liquids and gases, therefore, cannot be distinguished by symmetry. This reflects the fact that one may move continuously from a liquid to a gas phase simply by going around a critical point. All other equilibrium phases of matter are invariant only under certain subgroups of the Euclidean group and, therefore, have lower symmetry than fluid phases. This reduced symmetry is the cause of the ordered structures which are introduced in other phases. As a result, certain positional and rotational long-range orders are introduced in these phases. One example is an intermediate state such as a mesophase state. This proposition describes a class of materials which possesses order in between two extreme forms of condensed matter: homogeneous, isotropic liquids with an average structure that is invariant under arbitrary rotation and translation, and crystalline solids with average structures that are invariant only with respect to certain discrete lattice translations and point group operations comprising the space group. On the other hand, *mechanics* can be used to express atomic or molecular motions and interactions by providing a series of differential equations. However, this method can only solve problems considering motion and interactions among a few bodies. For a system which contains a large number of atoms or molecules, a mechanics approach does not yield analytical results.

Instead of microscopic parameters, temperature (T), pressure (P), enthalpy (H), entropy (S), free energy (F) and other macroscopic variables as well as material parameters may be used to describe a system based on *thermodynamics*. The basis for this kind of description comes from a few empirical laws (the three laws of classical thermodynamics) such as the conservation of energy, the fact that heat cannot be transferred spontaneously from a low T body to a high T body, etc. To establish a relationship between these two descriptions, one has to understand that the macroscopic thermodynamic description of a system is an *average* of the microscopic mechanical motions and interactions of the atoms or molecules. As a result, *statistical mechanics* serves as a bridge which connects these two descriptions.

* To whom correspondence should be addressed

To practically describe a phase, we need information containing a *structure function*, which represents the average relative positions of the atoms or molecules. For this purpose, we can define a *number density operator* which serves as a starting point for the definition of a phase[1]. This concept specifies the number of atoms or molecules per unit volume at a three-dimensional position $\boldsymbol{r}(x,y,z)$ as $n(\boldsymbol{r})$. The ensemble average of the density operator is the average density $< n(\boldsymbol{r}) >$ at $\boldsymbol{r}$. In homogeneous, isotropic fluids, this is the ratio between the overall number of atoms or molecules and the system volume. This indicates that $< n(\boldsymbol{r}) >$ is independent of both the magnitude and direction of $\boldsymbol{r}$ in the system, which is a reflection of the fact that the fluid is rotationally and translationally invariant. This high symmetry does not exist when the system is a crystalline solid or a mesophase. For instance, in a perfect crystalline solid, the number density operator is periodic, and the atomic or molecular density is invariant only with respect to translation through a lattice vector.

This structure function can be obtained experimentally via scattering methods. It is, in theory, a Fourier transform of the *correlation function* of the atomic or molecular density. Correlation functions of the density are ensemble averages of the products of the density operator at different points in space. There are several versions of the density–density correlation functions at different positions $\boldsymbol{r}_1$ and $\boldsymbol{r}_2$ which are commonly used. One frequently used function incorporates the difference between $< n(\mathbf{r}_1)n(\boldsymbol{r}_2) >$ and $< n(\boldsymbol{r}_1) > < n(\boldsymbol{r}_2) >$, and is known as one of the Ursell functions. It is important to note that the correlation function can be reconstructed from the structure function only if the correlation function is invariant with respect to position, as in the case of homogeneous fluids. Since periodic solids do not meet this criterion, they require diffraction methods to obtain the correlation function. It should also be noted that construction of a density operator from a correlation function is impossible.

The definition of phase transitions based on classical equilibrium thermodynamics was first proposed by Ehrenfest in 1933[2]. This macroscopic classification is based on the continuity of the thermodynamic free energy (F) and its derivatives. The first derivatives of the free energy are P (or V), S (or T), and polarizability. Their second derivatives are compressibility, expansivity, heat capacity and dielectric susceptibility. This Ehrenfest classification states that a *first-order transition* is defined as one in which the free energy is continuous (the Gibbs F in a T-P ensemble, the Helmholtz F in a T-V ensemble) but the first derivatives of the F are discontinuous. This implies that at the transition T, the thermodynamic functions at constant P or V exhibit discontinuous changes.

In a more general form, a Kth order transition can be defined as one in which all of the $(K-1)$ derivatives are continuous and the Kth derivative is discontinuous. In fact, this classification is not necessary, since in reality we generally experimentally observe only first-order (crystallization, crystal melting, most liquid crystal transitions, etc.) and second-order transitions (the critical point of a transformation between liquid and gas phases, superfluid and superconducting transitions without an external magnetic field, several ferromagnetic phase transitions such as Curie point, etc.). However, a few specific two-dimensional systems, multiple (more than two) fluid phase mixtures (such as tricritical, tetracritical or pentacritical points etc.), and theoretical predictions (such as the Bose–Einstein condensation in an ideal Bose gas etc.) may exhibit higher than second-order transitions. For simplicity, a first-order transition can be recognized as a *discontinuous transition*, and second- or higher-order transitions may be classified as *continuous transitions* or *critical phenomena*.

If we review some simple facts about phase transitions, it can be found that the degree of order and its corresponding symmetry change at the transition point. Generally speaking, a high-T phase usually possesses a relatively low degree of order with a relatively high symmetry, while a low-T phase shows the opposite trend. The concept of an *order parameter* ($< \Phi >$)[3] can be used to describe these changes at phase transitions. Therefore, at high Ts, the $< \Phi >$ can usually be defined as zero. At a critical T, T_c, order sets in, and below this T the $< \Phi >$ is nonzero. If $< \Phi >$ rises continuously from zero, the transition is a continuous transition (second-order). However, if it jumps discontinuously to a nonzero value when T lowers through T_c, the transition is first-order.

From a macroscopic point of view, at a given T and P thermodynamics dictates whether a phase transition is intrinsically possible. A complete understanding of the phase transition behaviour can be achieved using a *phase diagram*. A phase diagram is a particularly defined intersect plane in a three-dimensional *phase space*, such as the T-P plane. A phase diagram consists of several elements: points, lines and surfaces. Among these elements, the surfaces represent the conditions under which a specific phase exists. The lines are more attractive to study since they describe the discontinuous changes of thermodynamic functions of the phases and metastable behaviour. The isolated points are also of interest, specifically the critical points (both simple and multicritical). A phase transition which passes through a critical point does not involve V and H changes. The coexistence of two phases and metastability are not found at the critical point, and the isothermal compressibility and other physical parameters are possibly divergent.

Although microscopic descriptions of each phase are known, experimental measurements on transformations between two phases are based on observations of the changes of certain macroscopic material parameters with T and time. We thus need microscopic models to explain the observed data. In the area of crystallization, for example, normal and continuous crystal growth are two different descriptions of how molecules crystallize into an ordered state with or without a nucleation barrier.

In what follows, we shall first provide an overall survey of classes and manifestations of metastable states in which we shall transgress the boundaries of classical concepts. In subsequent sections we shall then provide specific examples for the cases cited in the general sections which have been taken from the polymer field and mostly from our own experiences.

CLASSICAL METASTABLE STATES

The metastable state is an important concept in condensed matter physics which has been recognized for a long period of time[4,5]. Due to its frequent dominance in phase transformations it was given specific attention as far back as the end of the last century when Ostwald formulated his '*stage rule*'[6]. According to the Ostwald stage rule, a phase transformation from one stable state to another proceeds via metastable states, whenever such exist, in stages of increasing stability. This rule was documented by an abundance of experimental observations. However, this

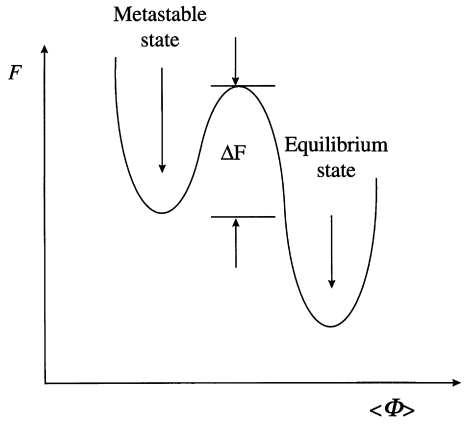

Figure 1 An illustration of a metastable state in a plot between F and $<\Phi>$. The ΔF is an activation barrier

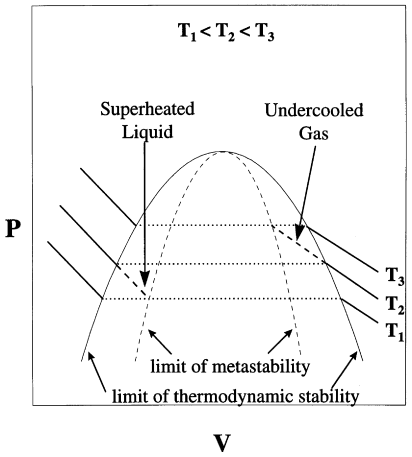

Figure 2 A relationship between P and V in a liquid–vapour transition system

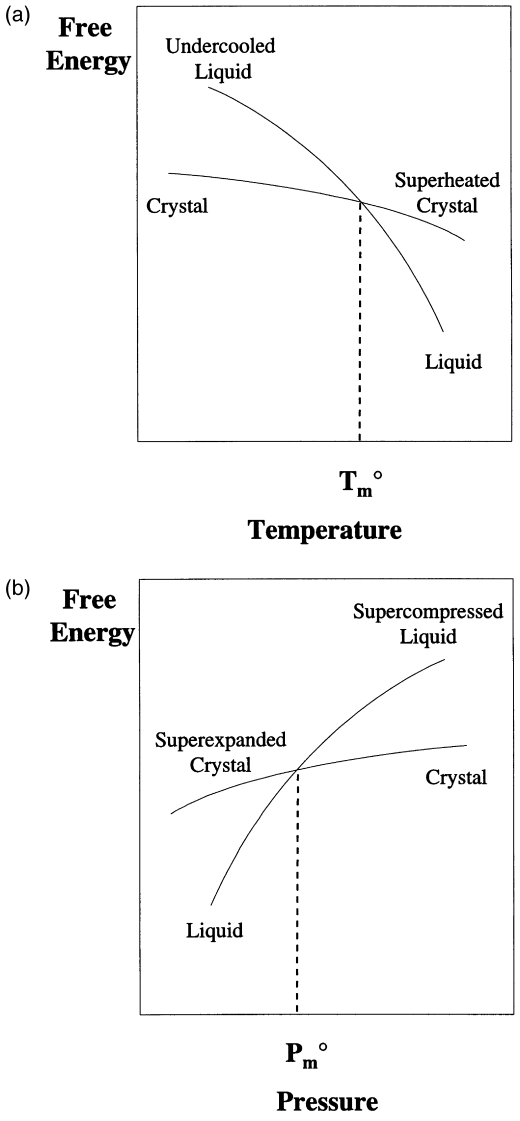

Figure 3 Schematic plots of (a) F *versus* T at a constant P and (b) F *versus* P at a constant T in the vicinity of a first-order transition

rule did not explain why this occurs, and was considered an intrinsic property of matter.

By definition, a metastable state is a state of matter which can exist based on the laws of thermodynamics and is stable with respect to infinitesimal fluctuation, yet does not represent the state of ultimate stability. Theoretically, in a plot of F *versus* $<\Phi>$, both metastable and ultimate stable states show that the first derivative of F with respect to $<\Phi>$, $dF/d<\Phi>$, is equal to zero, and the second derivative ($d^2F/d<\Phi>^2$) is positive. This can be clearly illustrated in *Figure 1*. Decomposition of the metastable state requires activation. Although the metastable state will enter an equilibrium state sooner or later, its lifetime must be longer than the time scale of the experiment, while the relaxation time of the atoms or molecules is much shorter than this lifetime.

A classical example of the metastable state is the condensation of a gaseous phase or the evaporation of a liquid phase between the *binodal* and *spinodal* lines where one may have a *superheated* liquid phase or an *undercooled* vapour phase. *Figure 2* illustrates the phase transition between the liquid and vapour phases. It is noted that below the critical T and P, the binodal line represents a first-order transition within the *limits of thermodynamic (absolute) stability* and the spinodal is the *limit of metastability*. This phenomenon was first described as early as 1873 by van der Waals in his well-known equation. In the practical application of this equation, the section $(\partial P/\partial V)_T > 0$ does not exist. When the system passes through the critical point, there is a second-order transition. However, at the critical point, liquid and vapour phases are not distinguishable.

A second example of metastability occurs in the vicinity of the first-order transition T for a crystal–liquid transition at constant P. In this case, a superheated crystal phase at a T higher than the transition T or an undercooled liquid phase at a T lower than the transition T may exist. This can be clearly seen in a plot of F *versus* T (*Figure 3a*) in the vicinity of a first-order transition. A similar illustration can also be seen in a plot of the F *versus* P at constant T (*Figure 3b*). These two plots can be viewed as two cross-sections of surfaces at constant P or T of a F-T-P three-dimensional phase space. The equilibrium transition T is the projection of a point at the phase boundary line.

In the phase planes of a crystal–liquid transition there can be no critical point since this would lead to disruption of the symmetry. The phase boundary lines extend towards infinity

or meet with other phases*. This behaviour is different from that of the liquid–gas transition described previously. As shown in *Figure 3a*, at constant P the F line of the crystal phase can be extended to higher Ts, and that of the liquid phase to lower Ts on both sides of the equilibrium melting T. This can also be found at constant T in a plot of the F-P plane as shown in *Figure 3b*. These F lines represent the free energies of the metastable states. There is a similar delineation between different possible variants of the crystal phase, termed *polymorphs*. In the case of polymorphism it is essential to realize that, unless we are at the intersection of the F lines, all but one of the possible polymorphs correspond to metastable states. At present it is not certain as to whether F lines associated with metastable states extend indefinitely as a function of T and/or P, or whether there are limits to the metastability in crystal–liquid or crystal–crystal transitions where the $d^2F/d < \Phi > ^2$ is no longer larger than zero.

When the limit of metastability is absolute (e.g. in the case of a spinodal, where such applies) this is determined by thermodynamics. However, in the majority of cases of phase transitions the limiting state is practically determined by the *kinetics*. In the classical metastable state, the question as to why the system can be trapped into a local F minimum, that is not the global minimum, can clearly be posed. The general explanation based on kinetics is that such a state is attainable at a faster rate. In terms of statistical mechanics, the atoms or molecules of the system have a larger probability (due to the limited average fluctuation amplitude) to chose a pathway which possesses a lower F barrier regardless of the thermodynamic stability after the barrier is overcome. In other words, these atoms and molecules are 'blind' and cannot predict the thermodynamic outcome behind the energy barrier. If most of the atoms and molecules are at a local minimum, a macroscopic metastable state forms which can be detected as long as the time and size scales of this state are compatible with those of the experimental observations. One may phenomenologically propose that during a transformation process, a metastable state may exist due to its fast kinetic pathway even though this state is thermodynamically less stable than the equilibrium state.

Considering liquid–crystal transformations in a single component system, a smaller barrier for the metastable state implies not only that the transition possesses a faster kinetics pathway at equivalent undercoolings (ΔTs), but also that lower ΔT is required for a practicably fast rate to be achieved when compared to the stable state. For making a comparison on an absolute T scale, we need to note that the upper stability limit of the metastable state is at a lower T, i.e. the metastable state has a lower melting point $(T_m)_{meta}$ compared to that of the stable state $(T_m)_{st}$. *Figure 4* illustrates the consequences for the overall phase transformation rates. Since $(T_m)_{meta} < (T_m)_{st}$, in the T region between $(T_m)_{st}$ and $(T_m)_{meta}$ (region I) the phase transformation always occurs directly to the stable state. However, when T is lowered to reach $(T_m)_{meta}$, the formation

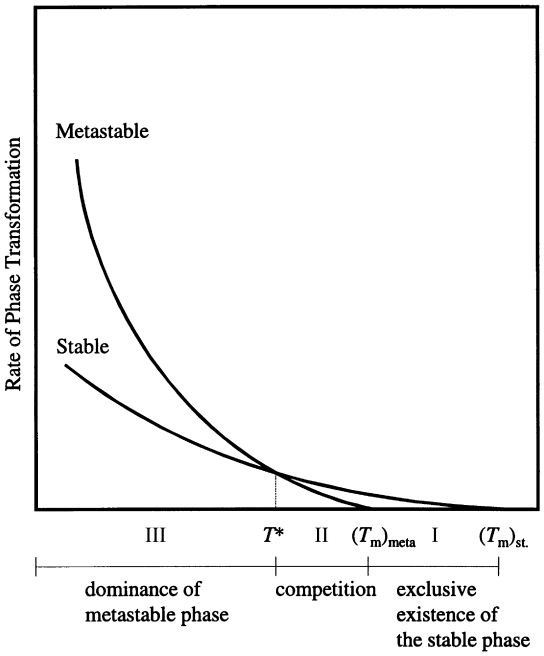

Figure 4 Curves for the phase transformation rates, R, as a function of T for the case where an alternative (*e.g.*, a polymorphic) phase can arise of which only one can be stable and the other is metastable, showing the mutual relation of the two rate curves on the same T scale. The curves cross over at T* defining three T-regions: (I) only the stable phase can form, (II) stable- and metastable-phase formation compete kinetically, and (III) metastable phase formation dominates[7]

rate for the metastable phase (R_{meta}) increases faster with decreasing T than the rate of formation for the stable phase (R_{st}). This results in a crossing of the two rate curves as shown in *Figure 4*. In general practice, this leads to the situation that when a liquid system is being cooled, the stability regime of a metastable solid (or mesomorphic) state can be reached before the ultimately stable phase had time to form. Therefore, on further cooling, the metastable phase will dominate the phase transformation with its more rapidly increasing rates. In fact, propositions to justify the Ostwald stage rule rest on such kinetic basis[7,8].

Specific examples in polymers will be provided in the coming sections. Polymers in general are highly undercoolable, in other words, they often require high ΔTs to induce crystal formation. As a consequence of the above considerations, *Figure 4* for polymers will acquire significance. In such situations, there is a strong possibility of entering the stability region of a metastable phase through quick cooling, even though it is deeply 'buried' beneath the phase of ultimate stability. The evolution of this metastable state takes place rapidly once its regime is reached. In fact, there can be more than one 'buried' metastable phase or even a whole spectrum of such phases forming a hierarchy of metastabilities where each one can evolve successively or in competition with others (see below) in compliance with the Ostwald stage rule.

Amongst different subject areas of condensed matter physics, one of the most intriguing and potentially far reaching example is that involving the phase behaviour of uniform colloidal latex particles in suspension. This is not only an important subject area in itself, but also can serve as a model for atomic and molecular phase behaviour including the role of metastability. As is well known, uniform spherical latex particles in the micrometer size range can form ordered three-dimensional arrays

* An alternative admissible possibility was envisaged by Tammann as early as 1903. Accordingly a solid–liquid phase line could also bend back on itself either forming a closed loop or terminating on the $T = 0$ and/or $P = 0$ axes. This would imply the existence of a reentrant melt phase (liquid or solid amorphous), *i.e.*, two melting points at a given P, which has not been given serious consideration. While not strictly pertinent to the present review it deserves a record at this place that, for the first time, an example has been found, and this is in the case of a polymer (Rastogi, S., Newman, M. and Keller, A. *J. Polym. Sci. Poly. Phys.* **31**, 129, 1993).

corresponding to colloidal 'crystal' lattices. Here, the 'crystal' forms through a first-order phase transformation with the concentration of the suspended particles as a variable. Recently, it has been shown that all three states of matter (i.e. gas, liquid, and crystal) can be represented by such a system, where the transitions often pass through metastable states and/or become locked into such states as defined in terms of bicomponent phase diagrams[9–11]. Note that for a hard sphere system the driving force is, in the first instance, purely entropic. However, through some recent ingenious developments, enthalpic interactions can also be introduced in a controlled manner which enables the mimicking of phase transitions in the widest generality. Specifically, the origin of metastable phases are being accounted for kinetically through the smaller energy barriers involved in their formation, with the concentration as a variable[12,13].

In the above colloidal systems the particles are spheres in a closely packed 'crystal' lattice. These systems of spherical entities have also received special attention through computational studies[14–16]. Currently, these are leading to the general result that the metastable hexagonal phase is the favoured polymorph compared to the face centered cubic structure of absolute stability. This is because the kinetic barrier to form the hexagonal lattice is smaller than that of the face centered cubic lattice. In fact, when the system size is sufficiently small, the hexagonal polymorph becomes the stable one, an important connection between phase size and phase structure. An additional point arising from these computations is that even crystals which are sufficiently large to exhibit the face centered cubic lattice should possess an outer shell of finite thickness with a hexagonal structure. Note that in the infinite size, this hexagonal structure is deemed to be metastable. At the time of preparing this review, there exists no experimental verification of this phenomenon. What more, rather surprisingly, there is no indication of any realization of the sweeping impact that this would have on the whole subject of crystal growth. Namely, if the above is true it would follow that during crystal evolution, the growth front is in the form of a different polymorph. Hence, the crystal would grow via a phase (structure) that is different from the one within the crystal interior. If the above computational results on closely packed spherical systems proves to be transferable to the lamellar crystals of polymers, the consequences this would have for our picture of chain-folded polymer crystal growth requires no elaboration.

Overall, for a metastable state to decompose towards an equilibrium state, a *nucleation* (which can be both *homogeneous* or *heterogeneous*) process must take place. Here again the kinetic rate at which critical sizes of nuclei are formed is entirely dependent upon the height of the F barrier which is determined by how deep the system is within the metastable region (ΔT). This process involves localized fluctuations with large amplitude. On the other hand, in cases where the decomposition towards an equilibrium state is by the spinodal mechanism, there is no F barrier involved. Here the equilibrium state spontaneously grows through long-wavelength (even macroscopic) fluctuations of small amplitude.

CIRCUMSTANTIAL METASTABLE STATES

Another class of metastability, which we have named '*circumstantial*', represents any state that has failed to attain its ultimate stability and may be arrested in one of multiple local minima in the F profile with respect to the $<\Phi>$ due to restrictions of the phase transformations. The stability of this state is associated with phase size and can be experimentally observed in the course of a slow transformation when compared on the time scale of our observations. Most, if not all, observable morphologies fall in this category, for which reason we shall use the term '*morphological*' metastability for this second category.

This broad class of metastability arises from the fact that in phase diagrams ultimate stability refers to phase dimensions which are large enough for the effect of surfaces on the stability to be negligible. In practice, the upper size limit where surfaces start having an effect depends on the system, but in general it is well within the micrometer scale. A phase domain limited to such small regions, such as dispersion of droplets in a liquid phase or a fine grain structure in a polycrystalline solid, is by definition metastable. These domains develop towards their state of ultimate stability, the single phase domain, by coalescence of the smaller phase regions (in other words, coarsening of the texture). This can be regarded as an ageing process, termed 'Ostwald *ripening*', which was identified long ago by Ostwald.

Under certain specific circumstances, the size of a phase can be intrinsic to the particular system. In an obvious case, the availability of material can be the size limiting factor (if there is not enough material a droplet or a crystal simply cannot grow larger). The newly forming phase remains small and the surfaces therefore have a consequential effect on the stability. Therefore, the minimization of the surface F (for the given small amount of material available) serves as the driving force to optimize the shape of the phase domain regarding its thermodynamic stability. In the case of a simple, free (unsupported) liquid, such a shape is a sphere, while in a crystal, the shape is the Wulff surface. All other shapes of the phase domain correspond to metastable states. This is particularly pertinent for the crystal case where the habits (shapes) may be determined by the kinetics of crystal growth rather than by the ultimate thermodynamic stability.

Other situations occur where small phase sizes can be found to arise in systems with specific inherent constraints. For example, there are block copolymers where the chemically distinct blocks within the chains segregate into separate (liquid) phases. These will intrinsically be microphases since the phase size is limited by the molecular connectivity. Complex and varied microphase morphologies can be obtained by the minimization of the overall surface F. These morphologies are thus true equilibrium phase structures[17,18], (in contrast to the morphologies we are dealing with in the rest of this review) and hence they are of no further concern here.

In what follows we shall be concerned with situations where there is an adequate reservoir of material, and no specific internal constraints are present so that there is no intrinsic obstacle to the attainment of a macroscopic phase domain, thus, the usual phase diagrams are applicable. In practice, nevertheless phase domains often remain small. In as far as the stability is affected by their small size, such systems are to be classified as metastable. In fact, we may state that the existence of a consequent morphology is a manifestation of metastability, hence the use of 'morphological metastability' in our terminology. This morphological metastability may have an increasing influence on the stability of the whole system as its scale falls into increasingly microscopic dimensions as is the case with polymers.

Polymers provide a rich field for examples of morphological metastability. Liquid–liquid (L–L) phase separation in polymer solutions or blends does not proceed to its state of ultimate stability (such as the formation of two layers, as does water and oil), but instead gives rise to varied arrangements of phase morphologies. These morphologies essentially fall into two classes according to the phase separation mechanisms of either nucleation or spinodal decomposition. In the case that the polymer is crystallizable, additional crystal morphology may arise within the phase morphology created by the L–L phase separation. Accordingly, there may be a hierarchy of morphologies, with a corresponding hierarchy of metastabilities.

In the case of L–L phase separation, a special point which needs to be made is the role of vitrification. A glass is usually in a non-equilibrium state, and hence is metastable. This metastability can be on two levels. First, there are materials which are capable of crystallizing but have failed to do so because of lack of mobility and thus remain in the glassy state. Such a glass is evidently metastable with respect to the crystals. Secondly, there are materials which are intrinsically uncrystallizable. Such a glass is also metastable, even if in this case only with respect to the liquid due to the excess volume usually associated with the glassy state. This makes such a glass metastable, moving toward its state of ultimate stability only very slowly. A more conspicuous manifestation of metastability associated with the glass state arises when vitrification interrupts a phase transition, thus 'locking in' the morphology that is prevailing at that stage. The phase transition in question can be L–L phase separation or crystallization, with the locked-in morphology corresponding to phase and crystal morphology, respectively. Experimental examples will be used as illustrations in subsequent sections.

Regarding the crystalline state, thermoplastic polymers, even chemically uniform homopolymers, are never fully crystalline, and in global terms they are characterized by an amorphous–crystalline ratio (termed *crystallinity*). This experimental fact on its own signifies the concept of the metastable state. Note that an equilibrium crystalline state below the crystal melting T corresponds to 100% crystallinity. However, in reality, these polymers have stopped crystallizing before reaching 100% crystallinity. There is no single local barrier which is responsible for this stoppage, it is rather a range of factors, essentially kinetic, which prevent the macromolecules from becoming fully incorporated into the crystals. The root of these factors lies in the long chain nature of the molecules. In structural terms, the so-called amorphous content comprises a range of states from localized fully amorphous domains to the surface regions of the small crystals with intermediate stages which can be characterized as strained amorphous and rigid amorphous.

The above-mentioned metastable states cannot be readily formalized or even defined in a unified manner. Nevertheless, there is one distinct and definitive structural feature which can be more precisely treated: the chain-folded lamellar crystal. This approach is not only important for the case of crystalline polymers, but also offers an opportunity for a quantitative discussion of size-induced metastability in service of a more general understanding of the phase behaviour in matter.

As is well known, the basic crystal units in a flexible chain polymer are lamellae containing the chains in a folded conformation with the lamellar thickness (ℓ) equal or related to the fold length (for a recent review see reference[19]). In an isothermal crystallization process, the primary crystal growth takes place along lateral directions with constant thickness (hence fold length), where the lamellar thickness is determined by the prevailing ΔT. This thickness is in the 10–50 nm range, and can be experimentally determined[20–23]. The small thickness of the lamellae lowers the crystal stability, thereby depressing the melting (or dissolution in the case of a solution crystallization) T and thus, in this sense the crystals are 'morphologically metastable'. The melting T depression associated with the crystal size can be expressed quantitatively through the Gibbs–Thomson relation[24] which, as applied to polymer crystals in the Hoffman–Weeks formulation[25], is

$$T_m = T_m^0\left(1 - \frac{2\sigma_e}{\ell \Delta H}\right) \tag{1}$$

where T_m is the melting point of the crystal of thickness ℓ, T_m^0 is the melting T of the ultimately stable crystal (i.e. for $\ell \rightarrow \infty$), ΔH is the heat of fusion, and σ_e is the surface F of the basal or fold-containing plane of the lamella (the effect of other side surfaces being considered negligible). It turns out that equation (1) is usually closely obeyed. This means not only that it can serve to assess crystal thickness, but also that such crystals can serve as models for verifying the validity of the Gibbs–Thomson relation, which is of much importance in the wider sphere of condensed matter physics.

The important issue is the reason for the formation of small phase size. This can include mutual impingement, external constraints, interruption of phase formation (say by vitrification of the melt), or simply very slow phase growth. In the case of chain-folded lamellar crystals in polymers however, there is an explicit kinetic barrier at a particular ΔT, and therefore a corresponding constant lamellar thickness is favoured for lateral growth. In general, this kinetically optimized thickness is defined through the nucleation barrier involved in the course of lateral crystal growth. In other words, each thickness could be considered as a distinct metastable structure: a morphological 'polymorph'. In this sense we suggest that this thickness determined 'morphological metastability' could be regarded as the first level of such metastability. This approach may be particularly pertinent to the chain-folded crystallization of long uniform oligomers, which only fold very few times and where the value of ℓ is quantized. This implies that ℓ is a small integer fraction of the chain length, suggesting that ℓ is not a continuous function of ΔT but varies in steps, making the corresponding crystals differ largely in thickness (examples of such systems will be presented later).

INTERLINKAGE OF THE TWO CATEGORIES OF METASTABLE STATES

In most of the practical cases of polymer crystals, classical and circumstantial metastable states are, of course, interlinked. Within the lamellar crystals, structures can be defined following crystallographic rules based on lattice symmetries. Thus, for a given polymer a range of polymorphs is possible in the conventional sense [say in polyethylene (PE) orthorhombic, triclinic and hexagonal crystal structures]. As described previously, in general all but one polymorph corresponds to metastable states. However, each crystal structure can be associated with different lamellar thicknesses as determined by the ΔT. We can thus have hierarchy of metastabilities, which are formed by interlinking one class of metastability related to the

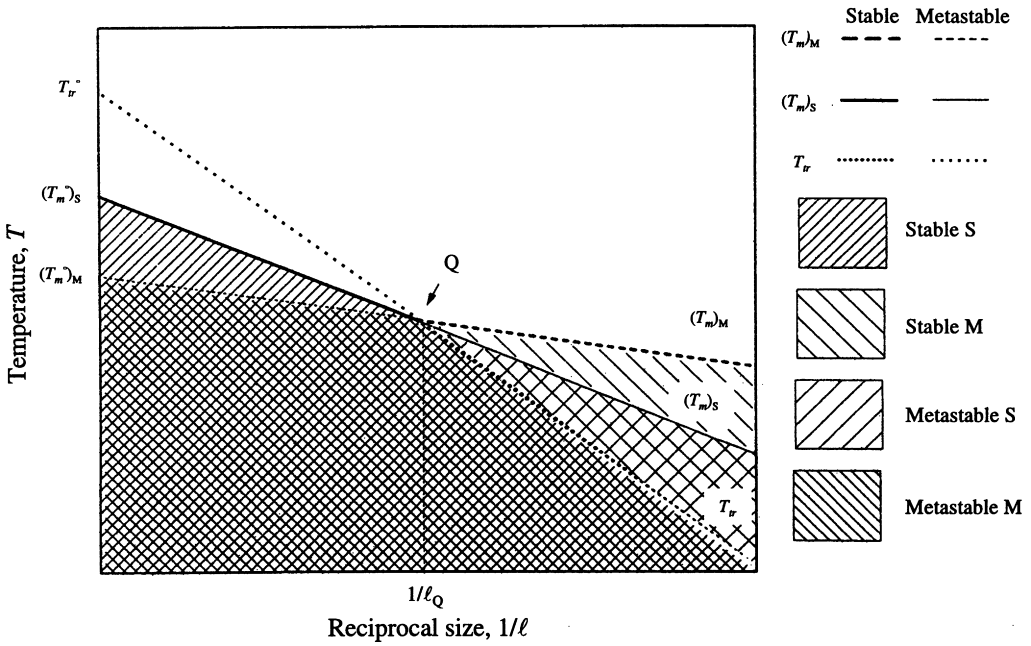

Figure 5 Temperature *versus* reciprocal size $1/\ell$, phase stability diagram obtained by plotting the T of intersection of Gibbs F *versus* size construction displaying the cross over of the phase stability with decreasing size. The S-phase melting is presented as a solid line, the M-phase melting is a broken line and the S → M transformation is a dotted line. The intersection of the phase lines defines a triple point Q, where all three phases (the melt, S and M) can coexist as stable phases. The different hatching, heavy for stable and light for metastable, denote the phase regimes where the S- and M-phases can exist either as stable or metastable phase[7]

lattice (classical metastability) with another related to the limited thickness (morphological metastability). Rather intriguingly, chain folded lamellae of polymers and uniform oligomers in particular, straddle the boundary of these two categories of metastability.

The above discussion implies that each crystallographic polymorph, as associated with the lattice symmetry, can be in the form of small crystals (as in the present case of lamellae). Therefore, each polymorph has its own size dependence according to equation (1). This size dependence may be different for each polymorph, as determined by the parameters σ_e and ΔH. Specifically, T_m will be a linear function of $1/\ell$ (see *Figure 5*) with T_m^0 as an intercept along the abscissa, and a slope of $T_m^0(\sigma_e/\Delta H)$. If two different polymorphs are possible (one stable and the other metastable), then, in view of the fact that $(T_m^0)_{meta} < (T_m^0)_{st}$ the T_m *versus* $1/\ell$ lines can cross over under a condition that $(\sigma_e/\Delta H)_{meta} < (\sigma_e/\Delta H)_{st}$†, which is a frequently obeyed inequality. In other words, we can have a conceptually important and, to our knowledge, not previously recognized situation where the stabilities *invert* with size. This suggests that a metastable phase defined by the classical metastable state can become the stable one when its phase dimensions are small enough, and conversely, a conventionally stable phase can become metastable when it is sufficiently small. This description can be understood from the construction of *Figure 5*. This possibility, i.e. *stability inversion* with size, as recently recognized, may have potential consequences for polymer crystallization[8,19,26].

If we consider the connection between thermodynamics (i.e. stability) and kinetics (i.e. rates) which emerges from size dependence, *Figure 4* may provide further information. The T_m *versus* $1/\ell$ lines in *Figure 5* represent the minimum phase size that is stable at each T. This implies that the polymorph which is stable down to the smallest size at a specific T will appear first in the course of isothermal crystal growth at that T. This smallest stable size is also the critical nucleus when approached from the viewpoint of kinetics. In turn, this critical nucleus represents the F barrier for crystal (or, in general, phase) growth: the smaller it is the faster the phase evolution. As stated in the preceding section, existing treatments of metastability, including attempts to explain the Ostwald stage rule, invoke the smaller barrier size and thus lead to faster rates as the reason for the prominence of metastable phase variants in phase transformations. We now see that due to the concept of stability inversion with size, the higher stability of the metastable phase (as referred to infinite size) in the case of small enough crystals and the faster rate of formation of this phase are interlinked. In fact, the two conceptions are equivalent, they are merely approached from two different viewpoints. Accordingly, a phase evolves preferentially in its metastable form not because of some inherent preference for metastability (Ostwald's implication) but because at its inception the metastable phase (due to its small size) had been the stable one, and at the same time (again, by virtue of its small size) the rate determining factor. It is then a question of whether such a phase will stay in the same form throughout its continuing growth. If so, the Ostwald stage rule will seem to be obeyed. Alternatively, it may transform into its state of ultimate stability, in which case the memory of the transient initial phase will be lost.

Another generality refers to triple points in phase diagrams when they are present, such as a triple point in a T-P ensemble (see below in *Figure 6* for PE) which, for sufficiently small phase dimensions, can become phase size dependent. This size dependent extension of the triple point into a 'triple line' was first treated by Defay *et al.*[27] in the case of a vapor–liquid–solid equilibrium. This treatment was also taken up in one of our laboratories[7]. A system consisting of the isotropic melt and two crystal structures (for example, the orthorhombic and hexagonal structures of PE) can be considered a truly three-component system.

† Generally speaking, the equilibrium transition $(T_m^0)_{st}$, differs only slightly from the $(T_m^0)_{meta}$ in terms of absolute Ts in Kelvin.

Studies on this system revealed an unforeseen singularity in the resulting expression for the size dependence of the triple point, indicating that the inclusion of size as a variable can have an even more profound effect than expected. This is potentially pertinent to phase behaviour in the widest generality. However, the physical meaning of this singularity has not yet been assessed, an issue that needs addressing.

Finally, the small phase size can also be a consequence of external constraints. The combination of reduced size and altered surface conditions may lead to a shift in phase stability that could result in an apparently metastable phase, as compared to conventional unconstrained macroscopic size. The word *apparently* means that just as in the case of purely size-induced stability shift, this phase is actually stable under the conditions of the external constraint, with the important difference that the constraints can usually be expressed in terms of thermodynamic variables and, hence, can be treated by true phase diagrams[28]. The constraints can be small cracks, gaps, or cavities in solids (the long studied classical case of capillary condensation is one example[28]). In polymer systems they can be the boundaries of microphases, e.g. phases which arise in block copolymers through localized liquid–liquid phase separation, where the material constituting the microphase is capable of further phase transformations such as crystallization or mesophase formation. These processes then have to take place within the preexisting confined microphase. Attention has recently been directed to this potentially important situation[29]. Another interesting example of constraints arises with polymer–clay composites. Here, polymers are intercalated between thin flakes of clay where the thickness of the resulting layers can be in the range of a few nanometers. There is a report on nylon–clay composites where the nylon is in a metastable crystal form[30]. While the authors of this report did not address it from the point of view of thermodynamic stability, we tend to interpret such observations as a consequence of a constrained size-induced shift in thermodynamic stability. In fact, because the clay layer separation is controllable, such systems should lend themselves to a systematic exploration of the phenomenon of size-induced stability inversion and also to the controlled production of metastable crystal polymorphs.

It is apparent from the above descriptions that the phenomenon of metastability is much more complex, and by the same token, much richer in variety than it may appear at first sight. This is our first attempt to place this entire subject in focus. Since the appropriate vocabulary is lacking to adequately describe the phenomena involved, newly proposed nomenclature, and the use of presently unavoidable, self-contradictory terms such as 'stable metastable' and 'metastable stable' are utilized. In this way, hopefully the subtly multifaceted diversity of the conceptual issues which are expressed by the nomenclature and definitions can then be translated by the reader into the correspondingly variegated effects and structures which arise in actual systems, and of which a few examples will be given.

POLYETHYLENE CRYSTALLIZATION: AN EXAMPLE OF PHASE INVERSION WITH SIZE

To recapitulate the relevant background, PE can exist as two crystal polymorphs in terms of conventionally defined crystal structure: the orthorhombic (*o*) and the hexagonal (*h*) phases (ignoring, for the present purposes, the mechanically-induced triclinic polymorph). These two crystal forms not only differ in terms of symmetry and

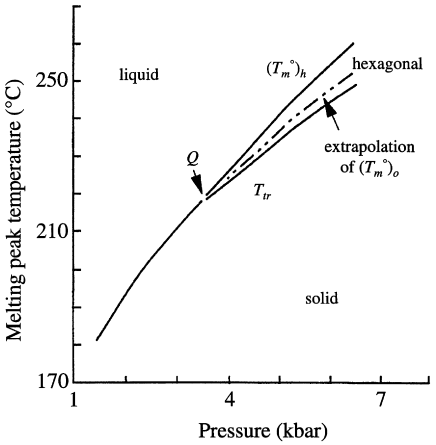

Figure 6 *P-T* phase diagram of PE displaying the appearance of a hexagonal phase beyond the triple point (Q). $(T_m^0)_o$ $(T_m^0)_h$ **are the melting points of the orthorhombic (***o***)** and hexagonal (*h*) phases and T_{tr} the $o \rightarrow h$ transition, all pertaining to infinite phase size (After Bassett and Turner, 1974[33])

atomic positions but, in a restricted way, also represent different states of matter. Namely, in the *o* structure the chains are in a crystal register, while the *h* structure is a mesophase with large molecular mobility along the chain direction. As a consequence of this distinction, the *o* phase is the representative structure of folded chains, while the *h* phase embodies extended chain crystals. In the former case, the crystals are growing only laterally with a fixed ΔT determined ℓ, while in the latter, the crystals also continue growing in the thickness direction ('thickening growth') and are terminated only by crystal impingement[31].

Originally, the *h* phase was recognized in experiments at high hydrostatic *P*[32]. The resulting *T-P* phase diagram is shown in *Figure 6*. Initially, it was found that the characteristic extended chain crystal morphology[34] arose upon crystallization in the newly recognized *h* phase regime[32]. However, it was subsequently observed that crystals can also start growth in the *h* phase also below the 'triple point' (T_Q), i.e. in the *o* phase region where the resulting *h* phase would thus be metastable[33]. Later studies[31,35] revealed that, slightly below the triple point, crystallization always started in the metastable *h* phase and proceeded in both the lateral and the thickness directions until an $h \rightarrow o$ transformation took place. In other words, a solid state transformation takes place from the less stable phase, *h*, into the phase which possesses the ultimate stability, *o* (*Figure 6*). At the same time, it was observed that crystal growth along both the thickness and the lateral direction stopped after the $h \rightarrow o$ transformation.

Figure 7 and *Figure 8* are illustrations of the above assertions from observations of *in-situ* polarized light microscopy (PLM). At this level of magnification only the lateral dimensions can be quantitatively measured while identifications of the *o* and *h* phases have been based on optical criteria combined with the results of *in-situ* wide angle X-ray diffraction (WAXD) experiments[31]. Both *Figure 7* and *Figure 8* show data points and visual images, respectively. The original untransformed phase (*h*), which is seen in the growth stage, begins to melt when *T* is raised to above the initial crystallization *T* (T_c). On the other hand, the transformed phase (*o*), which has stopped growing, remains unmelted. Thus, even without any reference to particular structures, this is self-contained evidence for the fact that the phase which starts and keeps growing is less stable, and hence is metastable compared to

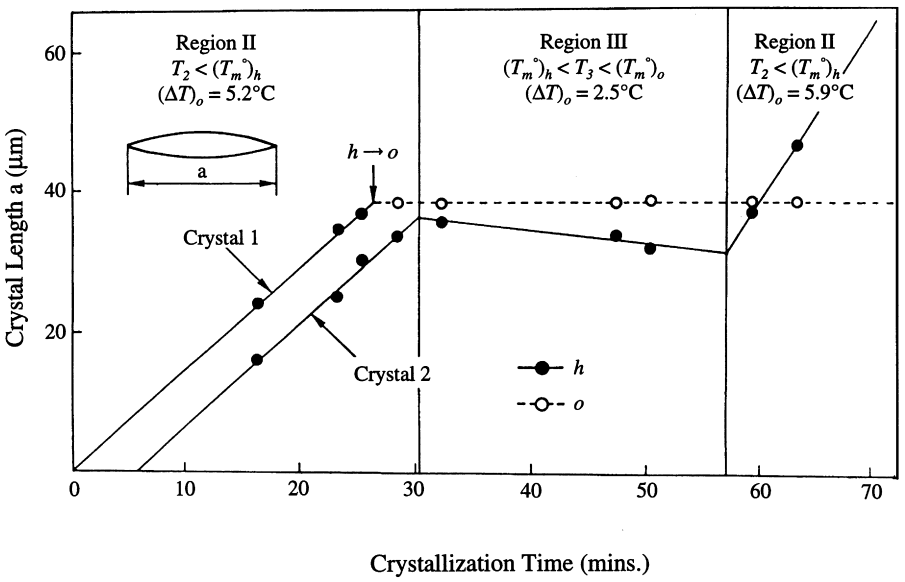

Figure 7 *In-situ* optical observation of length (a) of two crystals against crystallization time at $P = 3.2$ kbar. Temperature is varied during growth as indicated. After 26 min, crystal 1 (originally in *h* phase) transforms to the *o* phase and stops growing, while growth of untransformed crystal 2 continues in the *h* phase. After 30 min, the temperature is raised and crystal 1 (the *o* phase) stays unmelted while crystal 2 (the *h* phase) is slowly decreasing in size. Then, 28 min later, the temperature is lowered again, back nearly to where it was before. Crystal 2 (the *h* phase) resumes its growth, while crystal 1 (the *o* phase) remains arrested[31]

the phase which has ceased to grow due to a transformation. In other words, crystallization only proceeds in the metastable state (at least on the time scale of observation). In fact, as described in the previous sections on metastable states, *Figure 7* and *Figure 8* provide documentation that compared with the ultimately stable *o* phase, the metastable phase (*h*) possesses higher stability at its initially small size and also grows at a faster rate. This higher growth rate is the kinetic counterpart of the higher stability. Therefore, this observation certainly accounts for the Ostwald Stage Rule, and above all, comprises the phase stability inversion effect itself.

These PE results are unambiguously documented for the phase growth along the lateral direction. They can equally be applied to growth in the thickness direction through quantitative measurements in transmission electron microscopy (TEM) even if the PLM images have made this already qualitatively apparent. The explanation of this thickening growth behavior requires the introduction of size (ℓ) as a stability controlling factor which has appeared in the previous Sections. We shall now apply this principle to the special case of PE‡.

‡ By a number of indicators, lateral and thickening growths are interrelated, and this requires further exploration. In reference [7], a scheme was presented which allows for growth of an isolated lamella by one of two possibilities: lateral and thickening growth cease simultaneously (*Figure 7* and *Figure 8*), or lateral growth continues with constant thickness (usual crystallization). In the latter case, this is determined by the crystal geometry, specifically by the wedge angle at the growth front. We have also observations (unpublished) that, in a *T* and *P* region which is somewhat lower than that pertaining to *Figure 7* and *Figure 8*, a lateral crystal growth continues after cessation of the thickening growth (following the $h \rightarrow o$ transformation) through branching of the lamellae. Finally, recent measurements of the ratio of lateral to thickening growth rates suggest that most of the incremental material constituting thickening growth enters through the lateral faces of the crystal. This provides an explicit connection between lateral and thickening growth (Hikosaka, M., Amano, K., Rastogi, S. and Keller, A., *Proc. Int. Polymer Sci. Symp. for Prof. T. Kawei's 70th Birthday*, ed. A. Shagi and N. Okui, 1994, pp. 45–50). In the case that the flat-on lamellae impinge as a result of thickening growth while still in the *h* phase, the stage of $h \rightarrow o$ transformation will not be reached and the whole lamellar stack (with the exception of the two outermost layers) will continue to grow laterally in the *h* phase [31]. All these are clearly important new phenomena in polymer crystal growth, which, however, cannot be pursued further within the framework of this review.

The conception of stability inversion, which has been expressed in *Figure 5*, becomes readily applicable to PE if the phases to be referred to as stable (S) and metastable (M) are taken, respectively, as the *o* and *h* phases. The stability determining dimension ℓ is taken as the lamellar thickness. *Figure 9* illustrates isothermal crystal growth in terms of a phase stability diagram with notation appropriate to PE. First, one should note the fact that stability inversion with size applies only below the cross-over *T*, T_Q (a 'triple point' temperature). Above T_Q, the ultimately stable phase, which is the *o* phase in PE, appears and grows in the conventional way. However, below T_Q, the phase which evolves first for PE is the stable *h* phase due to its small size (note that the *h* phase is metastable when it is of infinite size). This small size is the kinetically defined critical nucleus. As the *h* phase grows along the thickness direction, it passes into the regime of the *o* phase, gaining ultimate stability upon attaining the size ℓ_{tr} (the thickness at which the $h \rightarrow o$ transformation occurs). It is dependent upon the kinetics of the solid state transformation. Two alternatives arise to be recapitulated. First, there is no solid state transformation on the experimental time scale and the end result is a macroscopic metastable crystal. Although this is possibly an explanation (or perhaps even *the* explanation) of the existence of metastable polymorphs in most simple substances, it certainly does not happen in PE: all existing experience teaches that the *h* phase cannot be 'quenched in', and the *h* phase always transforms into the *o* phase. Secondly, when growing past the size ℓ_{tr}, solid state transformation leading to the phase of ultimate stability does set in. Therefore, one expects that all traces of past growth history become obliterated, leaving no memory of the fact that the starting phase is different from the final phase. However, this last statement, while true for most crystals, does not apply to polymers such as PE. Namely, on the $h \rightarrow o$ transformation, thickening growth stops and the ℓ prevailing at the stage of the transformation becomes 'locked in' as a permanent feature of the morphology.

The above, when it applies, has two wider ranging consequences. One is that we have a morphological indicator of the genesis of the crystal marking the size

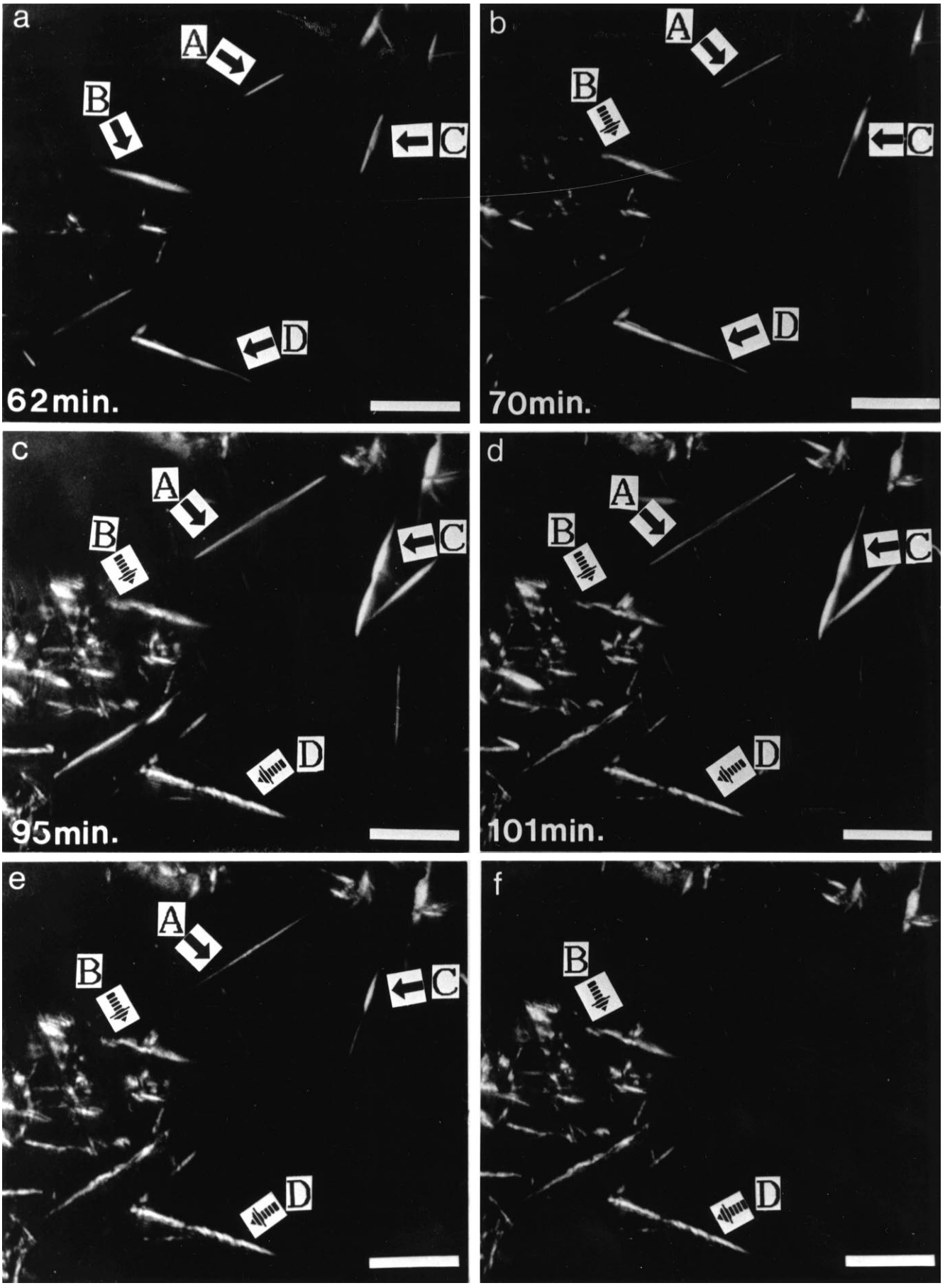

Figure 8 Optical micrographs as viewed between crossed polars displaying growth and melting behaviour of crystals at $P = 2.82$ kbar. (a), (b), (c), (d), show the growth of crystals at a fixed T, corresponding to the ΔT of 7°C for 62, 70, 95, and 101 min, respectively. (e), (f) show the melting of h crystals on raising the T, to $(\Delta T)_0 = 2$°C. Crystals marked $\rightarrow$ are in h phases whereas crystals $\Rightarrow$ are in o phase. Scale bar is 50 μm[31]

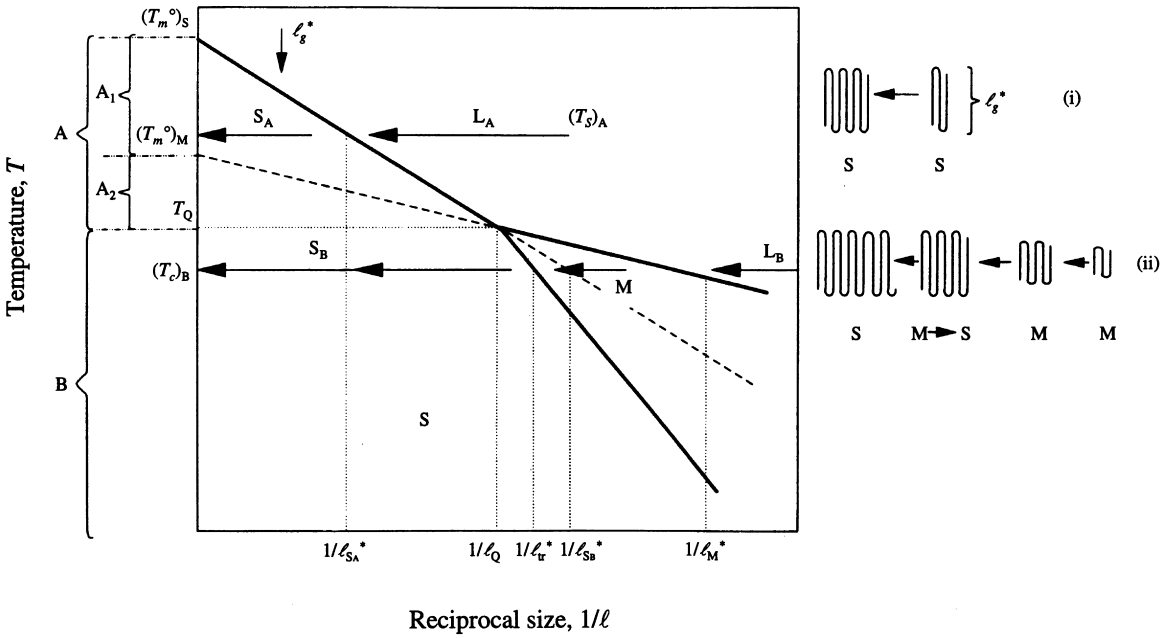

Figure 9 Phase (crystal) growth as a *T versus* reciprocal size, $1/\ell$, phase stability diagram, as in *Figure 5*. (—) Stable-phase demarcation lines, (– – –) metastable phase demarcation lines. (→) Pointing towards $1/\ell = 0$ denotes isothermal growth pathways at the selected (crystallization) temperatures, T_0. Two such pathways are indicated, one above and one below the triple-point temperature, T_Q ($(T_e)_A$ and $(T_c)_B$ which are representative of the growth regimes A and B, respectively). ℓ^* refers to the sizes of limiting stability (critical nuclei) of the respective phases. Schematic molecular illustrations are given of growth pathways for chain-folded polymer crystallization in (i) regime A, and (ii) regime B. Here (i) corresponds to the traditionally envisaged mode of growth, which is exclusively lateral at a fixed, kinetically determined thickness ℓ_g^*, where $\ell_g^* > \ell_{S_A}^*$, but it is now confined to region A; (ii) corresponds to simultaneous growth both in the lateral and the thickness directions (thickening growth); the latter is terminated by the M → S transformation somewhere along the arrow L_B in the C stability regime. The necessity of this mode arises in the newly recognized region B[7]

where it had changed structure, providing evidence that it had started growth in a structure that is different from the final one. The second consequence of particular importance for polymers is that it provides an explanation for the limited finite lamellar thickness of chain-folded polymer crystals. This will be clear from the sketches (ii) under region B in *Figure 9*. We emphasize that this need not be the only explanation and need not exclude the presently held views embodied by the kinetic theory of chain folding indicated by the sketches (i) under region A in *Figure 9*. In fact, the latter would apply, as before, at T_cs above T_Q and our new picture based on the $h \rightarrow o$ arrested thickening growth at T_cs below T_Q, the sketches (i), (ii) in *Figure 9* having been drawn and placed accordingly. It can be shown that the well documented $1/\Delta T$ dependence of ℓ follows from both mechanisms, and the two cannot be distinguished or tested on that basis alone[36].

As has been described in the previous Section, chain-folded crystal lamellae of limited thickness are metastable because of their small size in the thickness direction irrespective of the stability or metastability of the crystal structure contained in their interior. We draw attention again to the metastability hierarchy concept developed in the previous section. The present example is an illustration to show the intricate interplay between the stability–metastability characteristics on the different dimensional levels of structures in a way that is characteristic to PE and similar polymers. Namely, the interaction between the two different structure levels (traditional crystal structure and lamellar thickness characteristics) takes up a uniquely specific form. When the *h* structure is stable ('stable' for that size, ℓ) the crystal thickening growth will counteract the effect of size-determined stability until such growth ceases altogether as a result of the $h \rightarrow o$ transformation which takes place as the *o* regime is entered. Hence, the thickening growth, possible (or prevalent) only in one of the two phases, i.e. in the *h* phase (as defined on the level of the traditional crystal structure) is self-terminating which thus determines the phase structure on the larger dimensional level of the lamellar thickness.

At this stage the question as to the relationship of *Figure 5* (and *Figure 9*) to *Figure 6*, the true *T* and *P* phase diagram, needs to be raised. In fact, *Figure 6* is a section at $1/\ell = 0$ (i.e. $\ell = \infty$) of a general *P*, *T*, and $1/\ell$ phase stability diagram as shown in *Figure 10*. Alternative *T versus* $1/\ell$ phase stability diagrams such as in *Figure 5* and *Figure 9* are sections of *Figure 10* at $P =$ constant, where $P < P_Q$, P_Q being the triple point *P* in the conventional *P* and *T* phase diagram of *Figure 6*. *Figure 10* is in fact, the complete representation of phase stability with size (ℓ) [on the condition that the inequality $(\sigma_e/\Delta H)_{meta} < (\sigma_e/\Delta H)_{st}$ is obeyed]. We also see that the conventional triple point is extending into a 'triple line', and that the remarks on the unexpected singularities (arising from certain parameters) made in the previous Section apply.

Issues discussed above clearly call for experimental evidence. *Figure 7* and *Figure 8* are two examples of the extensive experimental material, parts of which are still unpublished. This material all relates to observations of the formation and melting of crystals by PLM, occasionally by WAXD, all *in-situ*, and by TEM. In the later case, the samples were quenched from T_c and removed from the crystallization *P* while within the *o* phase region of the *P-T* phase diagram for $\ell = \infty$ (i.e. *Figure 6*) to which *P* = constant and $< P_Q$ (the pressure at the triple point) sections in *Figure 10*, such as *Figure 5* and *Figure 9* apply. Even when $P < P_Q$ the experimental results which are available are still at elevated *P*. Clearly, extending such work to approach atmospheric *P* would be desirable in order to link up with the whole extensive body of work on the crystallization of bulk PE.

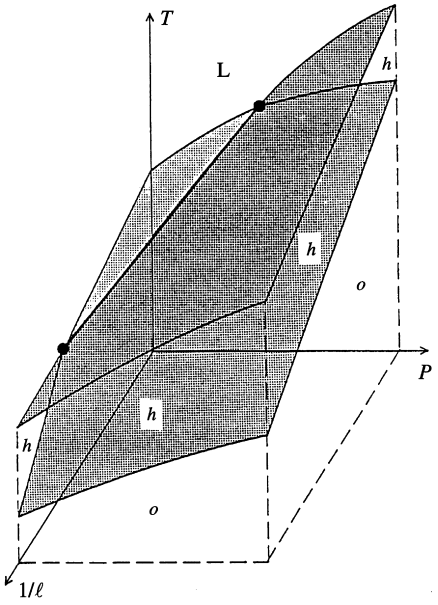

Figure 10 Combined three-dimensional T-P − $1/\ell$ phase stability diagram for a situation when *Figure 5*, *Figure 6*, and *Figure 9* would apply separately. The notation is potentially applicable to polyethylene (that is, S and M in *Figure 5* correspond here to *o* and *h* phases). The continuous shaded region (a volume in three-dimensional space) is a region where the intermediate phase (here *h*) is stable, connecting the corresponding region in *Figure 6* (infinite size) with those in *Figure 5* and *Figure 9* (finite size). The triple points become the extremities of a new *triple line*, which defines the boundary below which the *h*-phase can (or cannot) exist[7]

A somewhat different yet related approach aimed to provide support for the above evolved picture is to establish the existence of a stable *h* phase region in a $T - 1/\ell$ section of a P-$T - 1/\ell$ phase stability diagram such as in *Figure 5* and *Figure 9*. This is best done by heating pre-existing crystals of specified thickness (ℓ) and following their behaviour as a function of T by WAXD. It will be clear that for $\ell < \ell_{tr}$ the initial *o* crystal on raising T should transform into an *h* phase before melting. On the other hand, when $\ell > \ell_{tr}$, the *o* crystals should pass directly into the melt without any intervening *h* phase. Even if such experiments have not yet reached down to atmosphere P, they indeed have already produced the above-described results over a wide P range within $P < P_Q$[37]. On this basis alone, the reality of phase stability diagrams (such as *Figure 5* and *Figure 9*) and the existence of size induced phase inversion has been demonstrated.

One of the experimental problems which complicates the experimental observations, but at the same time provides further support to the whole picture, is that ℓ does not stay constant in the course of the heating experiments but increases. In fact, it is being found that such an increase sets in, or at least greatly accelerates, on entering the newly identified *h* region[37]. On the one hand, this is fully consistent with the expected high chain mobility in the *h* phase which induces (or promotes) lamellar thickening through chain refolding envisaged via sliding diffusion[38] (note that this corresponds to a secondary crystallization process, which is a perfection of the crystal already formed, in contrast to the previously considered thickening growth involving the addition of new material to the growing crystal). Such crystal thickening will move the experimental pathway from the initially chosen $\ell < \ell_{tr}$ towards $\ell = \infty$, particularly, once the *h* regime is entered. When ℓ becomes larger than ℓ_{tr} we are out of this *h* region, and will not re-enter it again on further raising of T, which, unless the WAXD recording is sufficiently rapid, will remain unrecognized. In the works just indicated[37], by using synchrotron *in-situ* WAXD, it has become possible to control and follow this increase in ℓ to a certain extent. In fact, it has been shown that when ℓ increases the *h* region could be exited (i.e. we have an $h \rightarrow o$ transformation when moving horizontally in *Figure 9*) and re-entered again (the $o \rightarrow h$ transformation when moving vertically in *Figure 9*) on continuing or renewed heating as long as ℓ remained smaller, hence crystals thinner than ℓ_{tr}.

Finally, we return to the wider perspectives indicated in the sections. By our terminology everything considered in the present section would count as 'stable'. Nevertheless, by rigorous thermodynamic definition referring to infinite size the *h* phase observed at P and T below the T_m^0-T_Q-T_{tr} (T_{tr} represents the transition temperature at which the $h \rightarrow o$ transformation occurs) line in *Figure 6* (hence, for $1/\ell = 0$ in *Figure 10*) would be classified as metastable, and so would be the full observational material referred to in the present section underlining the problem of terminology which arises in the description and even in the definition of metastability. Nevertheless, there are regions within the phase stability diagrams which are metastable by any criterion. These are defined in the legend of *Figure 5* (regions S and M there) with corresponding surfaces in the three-dimensional extension in *Figure 10* (not drawn in there). Such phase regions are truly metastable in the sense that they cannot be regarded as 'stable' with the demarcation between what is stable or metastable being merely shifted by size consideration or by externally imposed constraints. This has been the case in all the foregoing in this section and some other sections of this review. The distinction (i.e. between merely shifted stability–metastability boundaries and 'true' metastability) has, to our knowledge, not been purposefully recognized in the past.

We certainly accept that phases which are truly metastable without subject to external constraints and are of infinite (i.e. macroscopic) size do exist (such are, e.g. all conventional polymorphs) and without which Ostwald's stage rule would never have been formulated. Yet, as we have shown it is possible to consider such metastable phases as arising through a size-induced shift of stability in the initial stages of their evolution, as opposed to having some intrinsic preference to metastability. Without the recognition of such possibilities the role and importance of a truly metastable phase, as unrelated to any shift in stability criteria due to whatever cause and at whatever stage of the phase evolution, cannot be assessed or even adequately discussed. It is hoped that by at least raising these issues a step in this direction has been made.

INITIAL TRANSIENT STATES IN POLYMER CRYSTALLIZATION

Model systems for polymer crystallization are strictly uniform oligomers of increasing chain lengths. Such systems should make it possible to establish a continuity between the crystallization of simple chains such as conventional *n*-alkanes and true high polymers such as PE. Specifically, at what length do the chains start folding and in what manner? Such work, which in principle is the obvious starting point of polymer crystallization studies, was in practice, restricted by availability of suitable materials. Those available in uniform lengths were not long enough to fold, and those which did show folding were

far too long for this purpose and highly polydisperse. A suitable compromise, however, was found in the 1960s in the form of anionically polymerized low molecular weight (LMW) poly(ethylene oxide) (PEO) which could be obtained in the desired chain length range with sufficiently low degree of polydispersity to display at least the main features of truly monodisperse materials. Even though the monodisperse *n*-alkanes are available today through step-by-step organic synthesis, the results obtained on PEO still continuously serve as a mutually reinforcing example in this study. The specific efforts to be quoted here will first be on PEO, to be followed by one feature of relevance for the subject of the *n*-alkanes.

The most notable feature observed on PEO of MWs ranging from 2000–10 000 was that of integral chain folding (IF). Accordingly, the lamellar thickness (hence fold length), was not a continuous function of ΔT, such as with the usual high MW polymers, but varied stepwise, specifically increasing with decreasing ΔT and/or subsequent annealing, where the steps corresponded to the extended, once-folded, twice-folded etc. chain lengths. These results were first obtained by SAXS experiments[39–41], and subsequently by PLM and TEM. The latter two results further displayed some remarkable effects relating to morphology, crystal growth and crystal stability[42–48]. With the advent of the strictly uniform *n*-alkanes the IF behaviour became again apparent[49], where it could be unambiguously related to the now precisely known chain length. In addition, it was found that in the course of crystal evolution the IF crystal state was preceded by crystal thicknesses which were intermediate between those for the discrete IF crystal values. Therefore, these correspond to non-integral folded chain (NIF) crystals. The nearest IF thickness is finally attained through isothermal thickening or rather remarkably, thinning in isothermally conducted experiments. These latter results relating to NIF structures could then also be identified in the work on narrow LMW PEO with the effect including the subsequent thickening and thinning being examined. The works to be quoted here specifically are those on PEO. We now ask whether the chain molecules have been organizationally associated with each other, forming an IF chain conformation during crystallization, or whether they are 'blind' to the presence of other chains until their neighboring segments have crystallized. In the former case, the IF crystal forms directly from the melt. Otherwise, a NIF crystal appears as an initial *transient* state.

Our investigation involved several steps. The first step was to experimentally identify the *existence* of NIF crystals in PEO fractions via real-time synchrotron SAXS. Over a wide range of undercooling, NIF crystals formed initially, and then were transformed into IF crystals. Although the NIF crystal is thermodynamically less stable, kinetically it grows faster[50–57]. Compared to the IF crystals, the NIF crystals are morphologically metastable. *Figure 11* shows the formation of NIF crystals in a PEO fraction with MW = 3000 crystallized at 43°C as an example. It is clear that the NIF crystal having a fold length of about 13.6 nm appears first, which is in between the fold lengths of extended chain crystals [IF($n = 0$)] (19.3 nm) and once-folded crystals [IF($n = 1$)] (10.0 nm). The fold length of the NIF crystals is found to be crystallization T dependent, similar to the observed changes of fold length in polymer crystals (*Figure 12*) [54]. It is interesting to find that both *thickening* [NIF (IF($n = 0$) crystals] and *thinning* [NIF (IF($n = 1$) crystals] processes occur at constant Ts during the NIF → IF

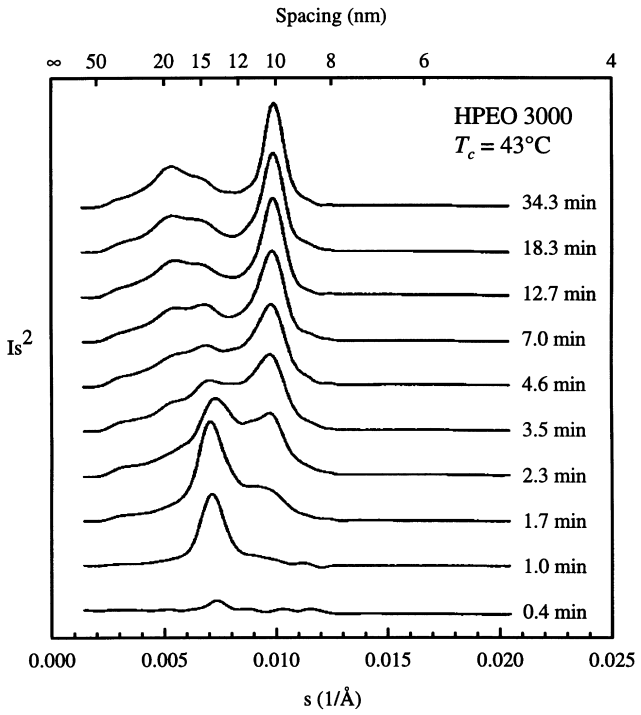

Figure 11 Set of Lorenz-corrected *in-situ* synchrotron SAXS data for a LMW PEO fraction with MW = 3000 at a T_c of 43°C for different times[54]

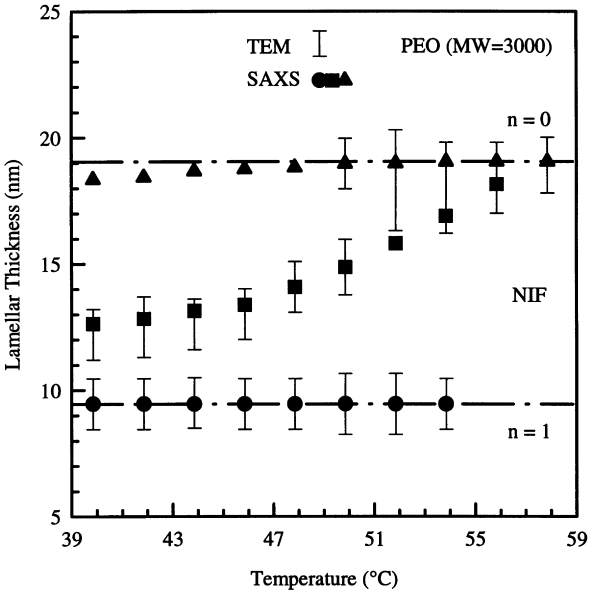

Figure 12 Set of NIF and IF crystal fold lengths at different T_cs for a LMW PEO fraction with MW = 3000[54]

crystal transformation. More importantly, these processes continue to occur long after the overall crystallization reaches completion [51,52,54–57]. The existence of the NIF crystals as well as these isothermal transformations have also been independently proven by Raman longitudinal acoustic mode experiments [58–61].

It is known that the size of crystals (such as lamellar ℓ) is critically associated with the crystal thermodynamic stability, and may obey equation (1). As a result, the thickening process is thermodynamically justified since the crystals are annealed into a more stable form. However, the thinning process in LMW PEO fractions is an issue

which needs to be further discussed, similar to the case of the *n*-alkanes[62,63]. When we think of thermodynamic and morphological criteria for these processes, one expects that if the Gibbs free energies of these crystals follow G(NIF) > G(IF, $n = i + 1$) > G(IF, $n = i$) and their fold lengths are l(IF, $n = i$) > l(NIF) > l(IF, $n = i + 1$), both thickening and thinning can take place [in the case of $i = 0$ and 1 it implies that there are IF($n = 0$) and IF($n = 1$) crystals]. On the other hand, if G(IF, $n = i + 1$) > G(NIF) > G(IF, $n = i$) and their fold lengths are l(IF, $n = i$) > l(NIF) > l(IF, $n = i + 1$), we return to the common case of polymer lamellar crystals in which the thinning process is forbidden. The explanation of the highest Gibbs F for NIF crystals is due to the inclusion of chain end defects within the crystals and the rough fold surfaces. Both factors destabilize the crystals and increase the Gibbs F of the system. Therefore, the NIF crystal is the least stable crystal among these three states even though it possesses a fold length which is thicker than that of an IF($n = i + 1$) crystal[56]. As a result, it can be understood that the F barrier to the formation of the NIF crystals must be the lowest among these three crystals and therefore, the LMW PEO molecules are trapped in this metastable state after the molecules overcome the NIF F barrier. Two F pathways exist for the NIF crystals to relax towards lower F states: one is the IF($n = 1$) crystal and another is the IF($n = 0$) crystal. The latter is the ultimate stable state among these three crystals. Furthermore, NIF crystals can also be found in the cases in which the fold numbers exceed one[55].

The study of the *MW dependence* of NIF crystal formation in these PEOs (MW: 3000–20 000) has indicated that with increasing MW, the transformation of the NIF → IF crystals is increasingly hampered by a decrease in the thermodynamic driving force between the initial NIF and the final IF crystals and an increase in the barrier to molecular motion. At sufficiently long chain lengths, the metastable NIF crystals may be permanently retained[56]. In polymers, the fold length shows a linear relationship with reciprocal undercooling as predicted by nucleation theory[64–69]. This could be consistent with the NIF state corresponding to a given ΔT with the retention of a well-defined morphological metastability. It must be stated, however, that this possibility cannot be readily distinguished from a situation involving IF in the case of long chains since it would give only very small incremental thickness changes imparting the impression that the fold length is a continuous function of ΔT.

Since these LMW PEOs possess —OH end groups, hydrogen bonding has been found in both the solid and the melt[52]. It has been speculated that the hydrogen bonding may play an important role in the IF crystal formation[70–77]. However, other end groups were also introduced into low MW PEOs, and IF crystals were still observed in many cases. We have systematically investigated the *end group effect* on the formation of NIF crystals and found that regardless of the type of end group, NIF crystals exist in LMW PEO fractions. Furthermore, the NIF crystals exist for a longer period of time as the end group size increases (from —OCH_3 to —$OC(CH_3)_3$ to —OC_6H_5)[52,57]. This suggests that a sliding motion of the chain molecules along the *c*-axis in the crystals may occur during and after crystallization. Larger end groups may hamper this kind of sliding motion, particularly in the solid state. This means that the existence of the metastable state is prolonged and thus the transient state can be readily observed even in conventional experiments.

In order to study the *effect of defects* at the center of LMW PEO fractions, we have designed two-arm PEO chain molecules with different arm lengths using 1,4-benzenedicarbonyl dichloride as a coupling agent[78]. For each molecule, both arms have equal lengths of MW = 2300 or 5500. Compared to linear PEO fractions with similar molecular lengths, the two-arm PEOs can be viewed as linear chains with a well-defined phenylene defect at the center of the molecule. The crystallization behaviour of the PEOs is monitored via WAXD, SAXS and DSC. Over a wide ΔT range, the two-arm PEO molecules do not appear to recognize the defects at the center of the chains during the initial stage of crystallization. During this stage of crystallization, they form NIF crystals having a fold length longer than the arm length. The defects are recognized only after the initial crystallization and gradually migrate to the lamellar surface through an apparent thinning process. This thinning process involves a transformation of the NIF crystals to crystals with two kinds of overall conformations for the two-arm PEOs, i.e. overall once-folded and extended chain conformations. The crystals containing these two overall conformations may also possess different stabilities. The crystallization kinetics of the two-arm PEOs are significantly slower than those of the linear PEO molecules having a length equivalent to a single arm as well as a combined length of two arms.

To end this section, a further effect is to be referred to first observed in a conspicuous form with the uniform *n*-alkanes[62,63], subsequently identified with the near monodisperse LMW PEO and currently acquiring wider generality as will be referred to again in a subsequent section. The effect in question concerns the rate of crystallization, both nucleation and crystal growth, individually and in combination. Instead of the customary smooth exponential increase with ΔT, the rates display a maximum followed by a sharp minimum as T_c is lowered, the minimum being in the T range where the once-folded chain crystallization (in the NIF form) takes over from the extended chain crystallization. This is being interpreted as a mutually interfering crystallization between the two crystal forms, the stable extended chain and the metastable once-folded chain crystallization. Since quite recently such a minimum was also seen at the crystallization T boundary between the once-folded chain and twice-folded chain regions[79], where now both forms are metastable with respect to the extended chain crystals, and the twice-folded form being metastable with respect to the once-folded one.

CLASSICAL CRYSTALLINE POLYMORPHS AND CONNECTIONS WITH MORPHOLOGICAL METASTABILITY

A number of polymers exhibit different crystalline polymorphs. At a given T and P only one of the polymorphs should be stable under equilibrium considerations (crystals with infinite size), and the rest of them are metastable in the classical sense. In reality, however, multiple polymorphs may appear under the same T and P due to rates of crystal formation and crystal sizes. Frequently, the metastable polymorphs can transform under proper thermal treatment conditions to more stable polymorphs. This may occur as a result of enhanced molecular mobility. In this section, we shall concentrate on the interlinks between classical polymorph metastability and size-dependent morphological metastability. Examples of polymorphs in polymer crystals can be found in PE (see previous section), isotactic polypropylene (the monoclinic α, the triclinic γ and the

hexagonal β forms), syndiotactic polypropylene (s-PP, the high T orthorhombic, the low T orthorhombic and the triclinic phases), *trans*-poly-1,4-butadiene (the monoclinic and the hexagonal phases) and many others.

The first example is s-PP crystallized at high temperatures, in which only size-dependent metastability is exhibited, while no polymorphs are seen. Over the past ten years, it has been found that the s-PP crystal structure with all *chiral* chain packing which was reported in the 1960s (cell I)[80] cannot be found in melt-grown lamellar crystals based on ED observations by Lovinger and Lotz. Instead, a fully *anti-chiral* chain packing model has been proposed, and the unit cell dimensions are $a = 1.450$ nm, $b = 1.120$ nm, and $c = 0.740$ nm (cell III)[81–84]. However, in s-PP WAXD fiber patterns, the cell I structure can still be recognized[85] (other polymorphs are also observed in s-PP samples, see for example a recent review[86]). It is known that at high crystallization Ts (low undercoolings), cell III crystals grow in s-PP samples. We have carried out a systematic study on the structure and morphology of highly faceted, regular, lath-like lamellar single crystals of s-PP fractions through TEM, atomic force microscopy (AFM) and ED[87]. Single crystals of s-PP larger than one micrometer in size can be grown from the melt in thin films. Although ED results obtained from the s-PP single crystals indicate the existence of the proposed unit cell III, the s-PP fractions can grow lamellar single crystals with two *micro-sectors* as shown in *Figure 13*. The A sectors are along the long axis (the *b*-axis) and the B sectors are along the short axis (the *a*-axis). Generally, at each crystallization T only one fold length can be found in lamellar crystals. Therefore, one way to observe the micro-sectors is to implement a method of PE decoration by which low MW PE crystals are oriented along the fold directions[88,89]. These micro-sectorized s-PP lamellar single crystals possess two different fold lengths with a ratio of around 3:2[87], which can be observed directly by AFM as shown in *Figure 14*. However, within one lamellar single crystal grown at a constant ΔT, the two micro-sectors should exhibit different metastabilities.

ED experiments have shown that the *c*-axis (molecular axis) of the s-PP single crystal is perpendicular to the substrate, and the crystal unit cell in both sectors are the same. The reason for this unexpected experimental observation of different fold lengths in these two sectors may be due to different fold surface free energies. The PE decoration method has been used to identify the chain folding directions[88,89]. In the A sectors, the chain folding is found to be parallel to the 010 direction. In the B sectors, little preferred orientation can be found. This is the same as in the case of non-sectorized s-PP single crystals[87]. From deformation of s-PP single crystals on a poly(ethylene teraphthelate) film, micro-fibrillar structures can be observed in the cracks of the single crystals along both the *a*- and *b*-axes after deformation (see *Figure 15*). This indicates that the folding direction in the B sectors may either be along the (110) planes or a combination of the (100) and (010) planes. Zigzag-shaped edges on the deformed single crystals along the *a*-axis are also observed and the sliding planes can be identified as the (110) planes[87]. This supports chain folding along the (110) planes.

The thermal stability of the crystals in these two sectors can be examined by melting the sector A crystals and retaining the sector B crystals. This can be realized using a temperature gradient method on the thin film samples. It is indeed found that the melting temperatures of these two

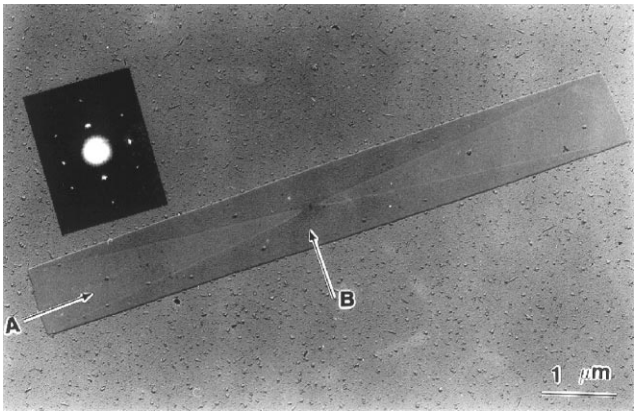

Figure 13 A lamellar single crystal of s-PP with sectorization[87]

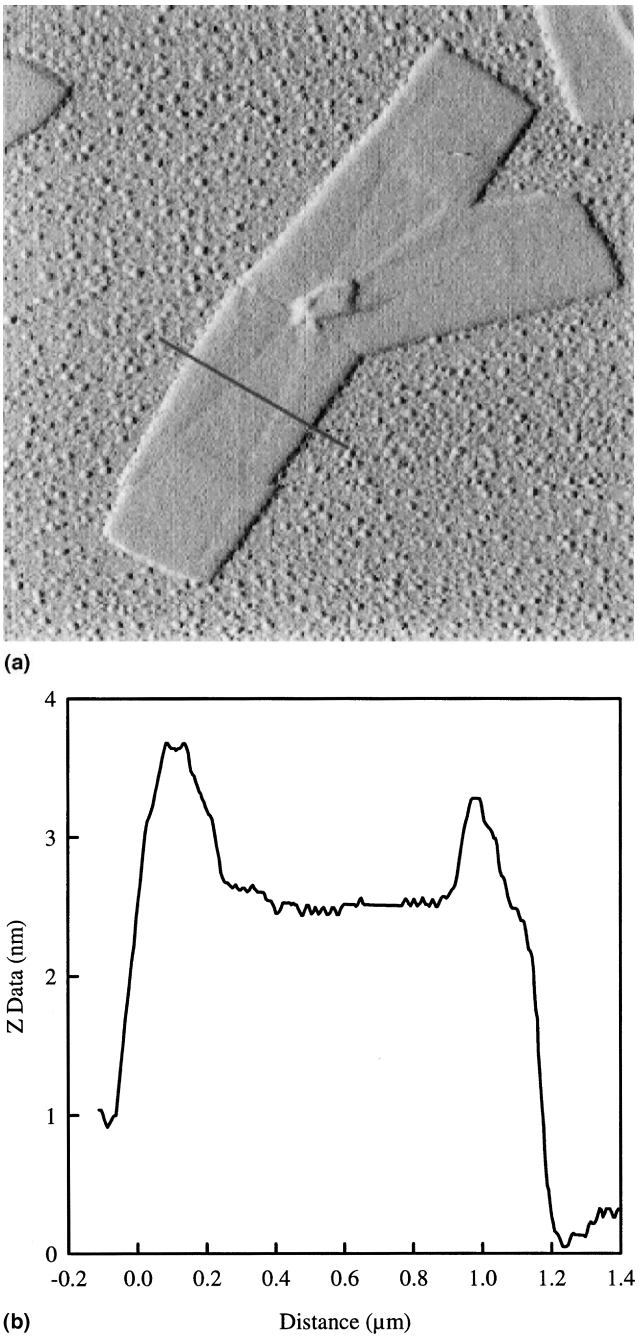

Figure 14 AFM micrograph of (a) sectorized s-PP single crystals and (b) a thickness profile of the single crystal along the solid line in *Figure 14a*[87]

sectors are a few degree apart[90]. This indicates that at a fixed ΔT, two different morphological metastable states are formed. However, it is still surprising that the different folding directions in the s-PP sectorized single crystal can cause such a drastic change of the fold lengths and therefore, different metastabilities. Therefore, we find a kind of 'morphological polymorphism' which possess the same lattice structure but different chain folding direction and thus, different folded surface F. This provides clear experimental evidence for the discussion in the previous Section.

The second example presenting the interlinks between the classical and morphological metastability is the case of poly(ether ketone ketone)s (PEKKs), which are high performance engineering materials. One member of this family is a PEKK with all *para*-linkages [PEKK(T)] which has the following chemical structure:

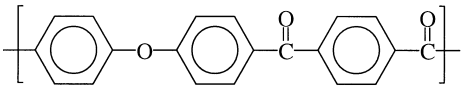

Previous work has shown that PEKK(T) has two polymorphs with different crystal structures (forms I and II)[91–94]. The form I structure was determined to have a two-chain orthorhombic lattice with $a = 0.769$ nm, $b = 0.606$ nm, and $c = 1.008$ nm (*Figure 16a*). Arguments were concentrated on the questions of the structural symmetry and unit cell dimensions of form II. Based on the same WAXD fibre pattern, two different symmetries and unit cell dimensions were determined: one was a one-chain orthorhombic unit cell with $a = 0.786$ nm, $b = 0.575$ nm, and $c = 1.016$ nm[91,93,94] (*Figure 16b*), and the other was a two-chain orthorhombic unit cell with $a = 0.417$ nm, $b = 1.134$ nm, and $c = 1.008$ nm[92] (*Figure 16c*). This occurred because the PEKK(T) WAXD fibre pattern showed too few reflection spots and therefore did not provide unique lattice symmetry and structure. The different symmetries of the two-chain and one-chain orthorhombic unit cells led to different reciprocal lattices and, therefore, were distinguished by ED experiments on lamellar single crystals (*Figure 17a* and *b*). After extensive effort, both form I and II lamellar single crystals of PEKK(T) have been obtained from the melt[95]. *Figure 18a* shows the morphology and ED pattern of the form I single crystals. The controversy surrounding the form II structure has been eliminated via ED experiments (*Figure 18 b*) in which the major crystalline planes were assigned. In this figure, the lamellar single crystal morphology is also included. Both forms I and II thus possess the $Pbcn$-D_{2h}^{14} space group in which the systematic absence of the reflections occur at ($hk0$) with $h + k =$ odd, ($0kl$) with $k =$ odd and ($h0l$) with $l =$ odd. For polymorphs and metastability respective of other members of this family see references[96–98].

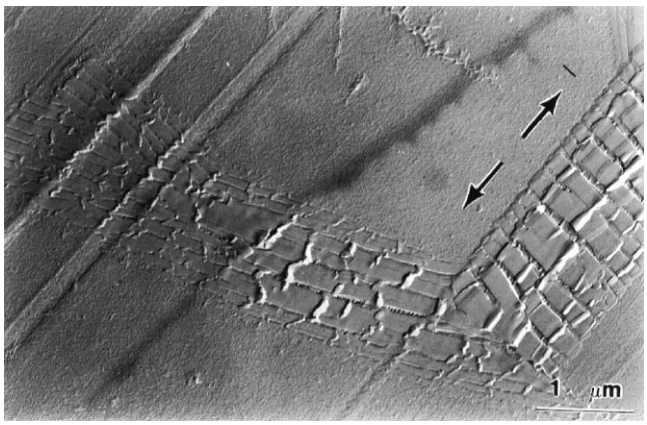

Figure 15 TEM micrograph of two deformed s-PP single crystals along both the *a*- and *b*-axes[87]

It is generally agreed that the form II phase forms only at relatively low Ts (high ΔTs) with limited molecular mobility and is metastable with respect to the form I phase which forms at high Ts (low ΔTs) and relatively high molecular mobility. Both forms should possess their own lamellar thickness dependence with ΔT and one form grows at the expense of the other. The formation mechanism of form II, which seems to compete with form I, is not completely clear. However, one may expect that in the low T region, the nucleation barrier of form II is lower than that of form I, while the opposite holds in the high T region. Although the exact T_M versus $1/l$ relationships have not been established, it is certain that the critical nuclear size of form II is smaller than that of form I and form II grows faster at high ΔTs than do the form I crystals. Since form II also possesses the orthorhombic lattice and molecular mobility in this phase is limited, the solid state transformation from form II to form I does not occur at least in the experimental time scale. Hence, form II can be observed as a polymorph even though

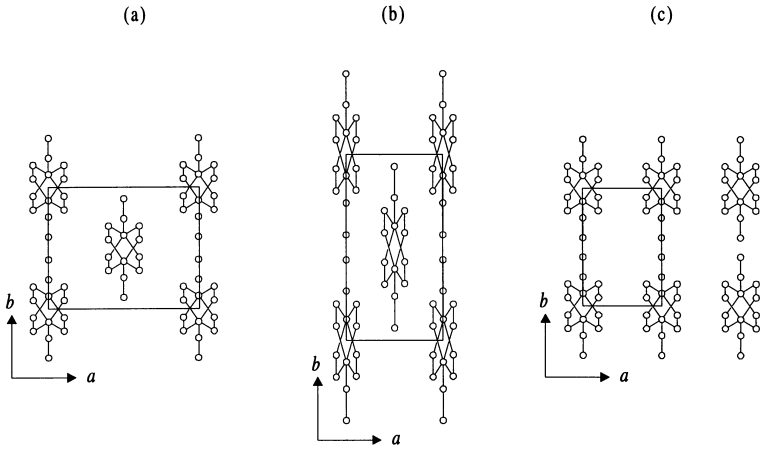

Figure 16 PEKK(T) crystal structures of (a) form I, (b) form II proposed in [91,93,94], and (c) form II in [92]

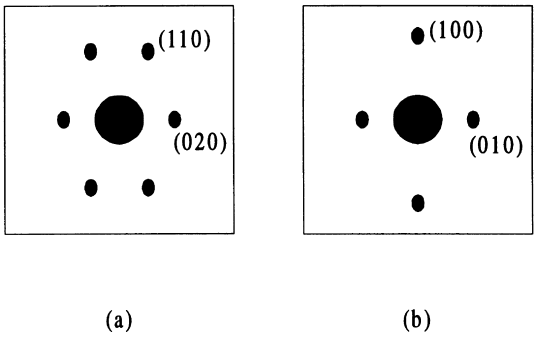

Figure 17 Predicted [00l] zone ED patterns for (a) two-chain and (b) one-chain orthorhombic form II structures[95]

it is a metastable crystal form. This system thus provides an example of the interlinks between crystal polymorphs (classical metastability) and crystal size (morphological metastability).

MONOTROPIC PHASE BEHAVIOUR

Two classes of phase transformation behaviours can be observed when more than one ordered phase exists in a system: *enantiotropic* and *monotropic*. Phenomenologically, the former represents a situation where both phases can be seen during cooling and heating, while the latter shows that two phase transformations are found during cooling and only the stable one can be observed upon heating. For a polymer system which contains both crystal and mesophase, such as a liquid crystalline phase, an enantiotropic liquid crystalline phase possesses thermodynamic stability in a T region between the T_m and the isotropization T (T_i). A monotropic phase, however, is metastable throughout the entire T range. Experimentally, it is only possible to observe the monotropic behaviour on cooling provided that the crystallization process is *bypassed* by undercooling due to the kinetically controlled nucleation process. It should be noted that this observation is only possible within the limits of metastability of this phase. The recognition of monotropic phases can be traced as far back as 1877[99]. From a thermodynamic point of view, one can readily understand the monotropic phase through a plot of the F of the different phases *versus* T as shown in *Figure 19a* and *b*[100].

In small molecule liquid crystals, a few samples have been reported which show monotropic behaviour[101,102]. When the mesogenic groups of these liquid crystals were used to synthesize polymers with methylene units connecting these mesogenic groups, the monotropic liquid crystalline behaviour may be retained. One example is 1-(4-alkylphenyl)-2-(4-cyanophenyl) ethane[101] and its polymer analogue, synthesized from a coupling of 1-(4-hydroxyphenyl)-2-(2-methyl-4-hydroxyphenyl)ethane and odd-numbered α,ω-dibromoalkanes (MBPE)[103–105], both of which show monotropic nematic (N) liquid crystalline behaviour.

It is particularly challenging to identify the monotropic phase. For a monotropic liquid crystalline phase, DSC and WAXD experiments using different cooling rates must be conducted in order to judge the nature of the transition (equilibrium *versus* kinetically controlled process). Specifically, the reason for the appearance of monotropic liquid crystalline behaviour is most likely due to the decrease in rigidity, linearity, symmetry and aspect ratio of the mesogenic groups. This leads to a reduction of the liquid crystalline phase stability, and therefore, a decrease in the transition T which may be mainly caused by an increase in the S term of the liquid crystal phase.

Monotropic liquid crystal behaviour also provides a practical opportunity for a study of crystallization behaviour from both the isotropic melt and the liquid crystal states. As

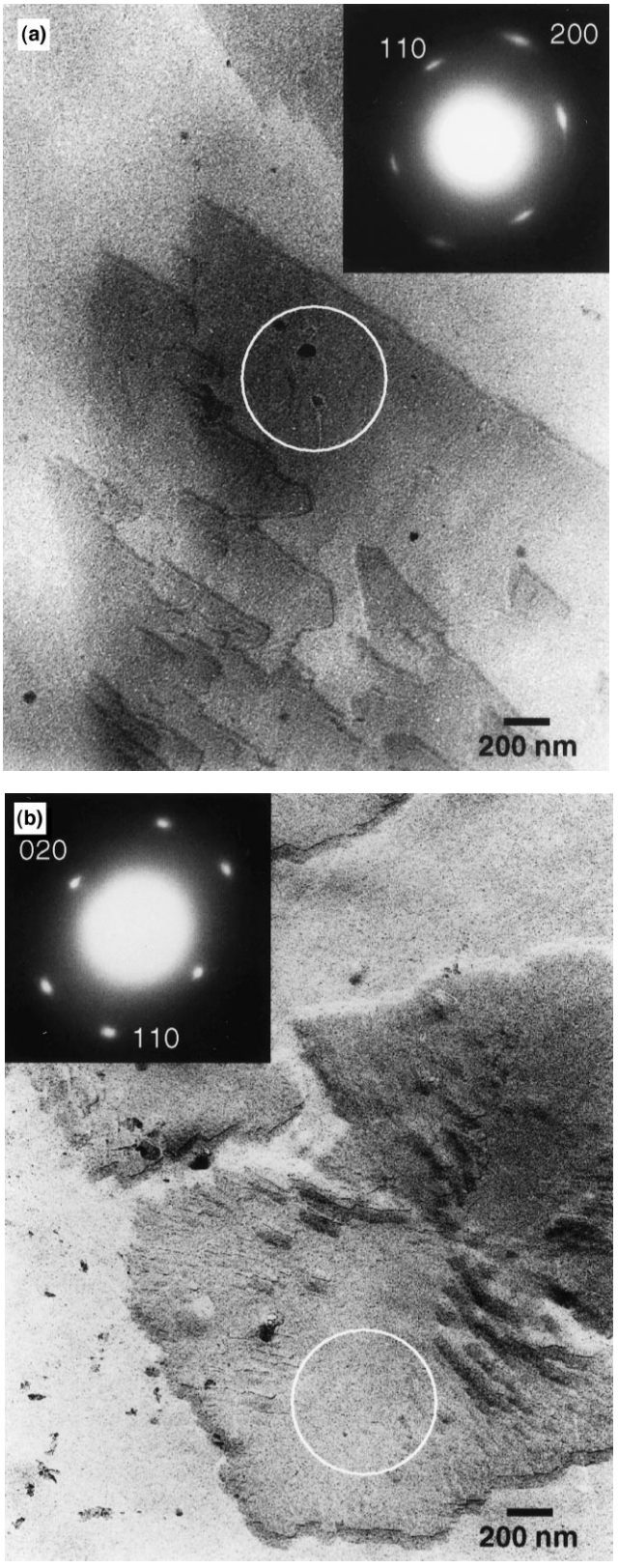

Figure 18 PEKK(T) single crystal morphologies and ED patterns of (a) form I and (b) form II[95]

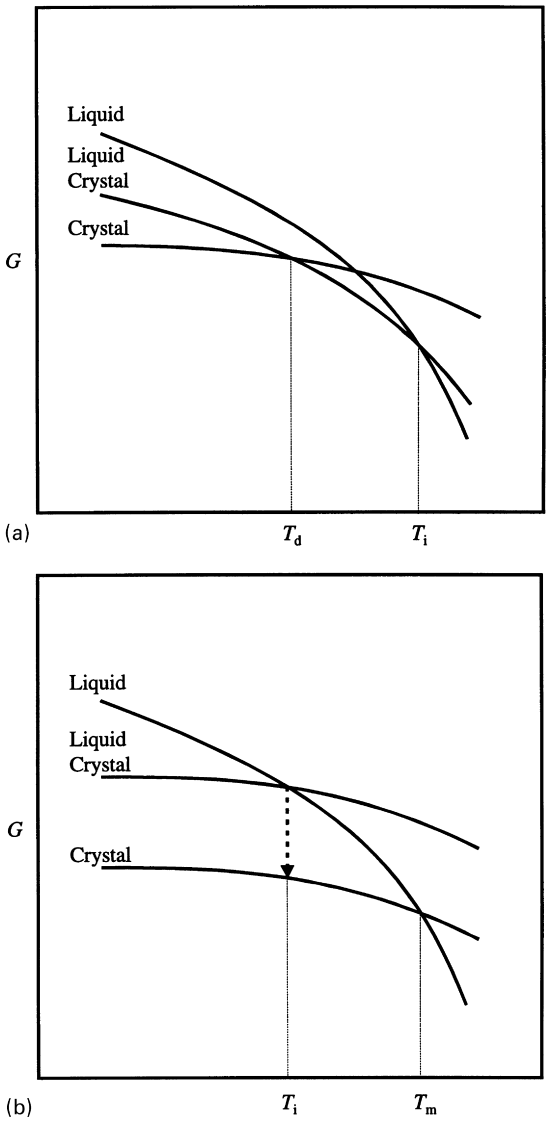

Figure 19 Thermodynamic Gibbs F changes for different phases with T: (a) enantiotropic and (b) monotropic behaviours[100]

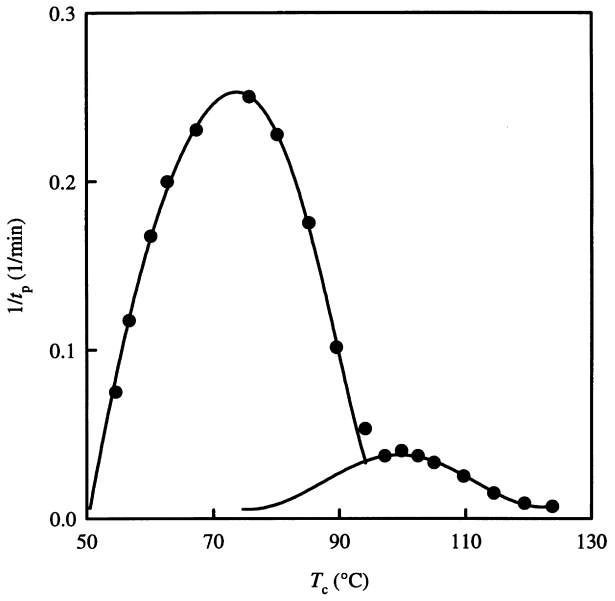

Figure 20 Overall crystallization rates for PEIM($n = 11$)[107]

described in *Figure 4*, three phase transition rates may be considered: a crystallization rate from the isotropic melt, a liquid crystal formation rate from the isotropic melt, and a crystallization rate from the liquid crystal state. Three kinetic regions for these phase transformation rates can be identified as shown in *Figure 4*: crystallization directly from the isotropic melt (region I), crystallization from the liquid crystalline phase in which the liquid crystal formation rate is much faster than that of crystallization (region III), and a crystallization rate which has the same order of magnitude as that of the liquid crystal phase (region II). Crystallization from the isotropic melt in region I is a nucleation-controlled process[106,107]. On the other hand, liquid crystal formations from the isotropic melt are near equilibrium transitions, and therefore, the transition kinetics are fast and difficult to trace experimentally[108–112]. However, our recent kinetic study of a series of liquid crystalline poly(ester imide)s synthesized from N-[4-(chloroformyl)phenyl]-4-(chloroformyl)phthalimide and different diols containing 4 to 12 methylene units [PEIM(n)][107,113,114] shows that the low ordered smectic phase formation may also be nucleation-controlled. Furthermore, when the monotropic liquid crystal transition T is close to its glass transition T (T_g) such as in the case of PEIM($n = 7$) which exhibits a 11°C difference between the liquid crystalline transition T and T_g. The liquid crystal formation kinetics are substantially slowed down due to hampered molecular motion. Times for 50% liquid crystallinity development in this polymer are in a range between a few minutes to an hour, which can be experimentally detected[107].

In *Figure 4*, the phase formation rates for both crystallization and liquid crystallinity from the isotropic melt are illustrated[7]. Under the condition that the crystal structures formed from the liquid crystalline phase and crystallized directly from the melt are the same (in some cases they are not), it can be understood that in region III, crystallization from the liquid crystalline state is actually a two-step phase transformation process from the isotropic melt to the crystalline state: a transition from the isotropic melt to the liquid crystalline phase followed by a transition from the liquid crystalline phase to the crystal phase. Since the monotropic liquid crystalline state is a metastable phase over the entire T region, it serves as an intermediate step in the crystallization process. One may predict that the crystallization rate from the liquid crystalline state should be faster than the rate of crystallization from the melt. This is indeed the case for a series of PEIM(n)s[107,113,114]. As an example, *Figure 20* shows the overall crystallization rates over the entire range of T_cs for PEIM($n = 11$). The existence of a pre-ordered phase (here, a S_A liquid crystalline phase) significantly enhances the crystallization rate in region III.

Region II in *Figure 4* is particularly interesting and deserves further discussion since in this region both crystallization and liquid crystal phase formation rates from the isotropic melt have the same order of magnitude. As shown in *Figure 4*, generally, the overall crystallization rate below $(T_m)_{meta}$ would be an additive function of the rates of the two individual processes, i.e. 'stable' and 'metastable'. In region II, the two rates are broadly comparable, with the metastable form taking over in region III. However, there is an increasing amount of evidence of a situation where in the vicinity of $(T_m)_{meta}$ the two processes can hamper each other. The rate minimum in the oligomers referred to earlier, displayed at the temperature near the stability boundary of the extended, once-folded states etc. were the first observations of such a

case. Since then, similar situations have been recognized in bicomponent systems comprising 'buried' phases, usually associated with the physical gelation phenomenon (see below). Namely, when passing below the phase line corresponding to the phase of ultimate stability, the rates of crystallization first go through a maximum decreasing until a virtual cessation of the process on further decrease of the *T*, shooting up rapidly again as the stability limit of the next stable 'buried' phase is reached and traversed. It seems to follow that such an initial hampering process between the formation of phases of different stabilities could be of wider generality inviting further attention.

SURFACE STABILIZED METASTABLE PHASES

Since the first discovery of the liquid crystalline phase over one hundred years ago, the classification of distinct liquid crystalline phases in small-molecule liquid crystals has been well established based on the types of order (long range, quasi-long range, and short range) in *molecular orientational*, *positional* and *bond orientational* order in different liquid crystalline phases[115–117]. Although some studies have shown that S_A, S_C, or higher ordered smectic phases may also be observed in polymers[118–123], traditionally, one hesitates when considering the existence of highly ordered smectic and smectic crystal phases due to the difference in connectivity between polymers and small-molecule liquid crystals. Despite this difference, we can show that highly ordered smectic phases may also be found in main-chain liquid crystalline polymers in a series of polyethers synthesized from 1-(4-hydroxy-4′-biphenyl)-2-(4-hydroxyphenyl)propane and α,ω-dibromoalkanes which are abbreviated as TPPs. The generalized chemical structure of TPP is[124]:

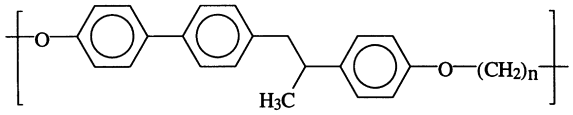

Phase diagrams of high MW TPP(n = odd)s regarding their thermal transitions are shown in *Figure 21*, as an example[125–127]. The transition *T*s in these phase diagrams correspond to near thermodynamic equilibrium since in this series of polymers these phase transitions show little ΔT (and superheating) dependence during cooling (and heating) experiments.

It is important to note that the concept of metastability can also be used to explain the phases and phase transition behaviour in *thin* films of these polymers on surfaces with different chemical and physical environments. The definition of a thin film is one in which the film thickness is on the same order of magnitude as the molecular dimension (say, ranging between 10 nm and 100 nm). Thin film induced phase stability was first reported in the 1980s in a few small liquid crystalline molecules[128–130]. Previously, this phenomenon had not been found in the case of liquid crystalline polymers. In our laboratory, a thin film surface induced new phase stability and ordering in TPPs can be found. This phase is metastable and cannot be seen in the bulk samples.

TPP(n = 7) bulk and fibre samples show three liquid crystalline phases: the N phase and highly ordered S_F and smectic crystal G (SC_G) phases (both of which possess a hexagonal lateral packing lattice)[125]. No SC_H phase is found (which has an orthorhombic lateral packing lattice). The SC_H phase in TPP(n = 7) bulk samples may thus be

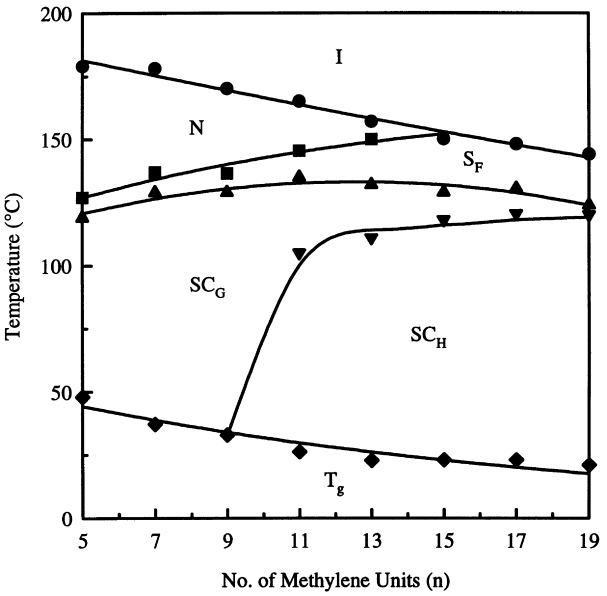

Figure 21 Phase diagrams of TPP(n = odd)s[125]

metastable and it is 'buried' beneath the T_g (*Figure 21*) in normal conditions. However, in the case of a thin film, the confined geometrical environment may provide additional stability to the SC_H phase and thus, this phase becomes observable. The detailed structure and morphology of TPP(n = 7) thin films has been studied by ED and TEM experiments on three different types of substrates. These include silane grafted, amorphous carbon coated and clean glass surfaces. The development of *homeotropic* molecular alignment in *monodomains* has been obtained by using substrates with silane grafted and amorphous carbon coated surfaces. Both surfaces can also induce structural ordering in TPP(n = 7) to form an orthorhombic lateral packing which does not exist in the bulk and fibre samples of the material in TPP(n = 7), and has only appeared in TPP($n \geq 11$). This phase has been identified as a SC_H phase. It has been found that the monodomain morphology of the highly ordered smectic crystal phases with homeotropic molecular alignment depends strongly on the structural symmetry. These results are shown in *Figure 22a* and *b*. It is evident that for a hexagonal lateral packing, the monodomain shows a circular shape while for an orthorhombic packing the shape becomes an elongated ellipsoid[131]. On the other hand, the clean glass surface does not induce orthorhombic packing and only polydomain structures can be found in which an in-plane *homogeneous* alignment of the chain directors exists. Mechanically sheared thin films on glass surfaces show uniaxial homogeneous molecular alignment.

This study indicates that the constraints of size and dimensionality, such as in the case of thin films on a substrate on polymer systems may effectively shift the phase stability boundary so as to stabilize a phase which otherwise would be metastable phase in bulk samples. Thus, for small film thickness, both free surfaces and interfaces, become increasingly important in the determination of the thermodynamic stability of the system as a whole.

TWO-FLUID SEPARATION AND VITRIFICATION

In this section, we introduce vitrification as an agency for creating metastability, not only through the glass usually

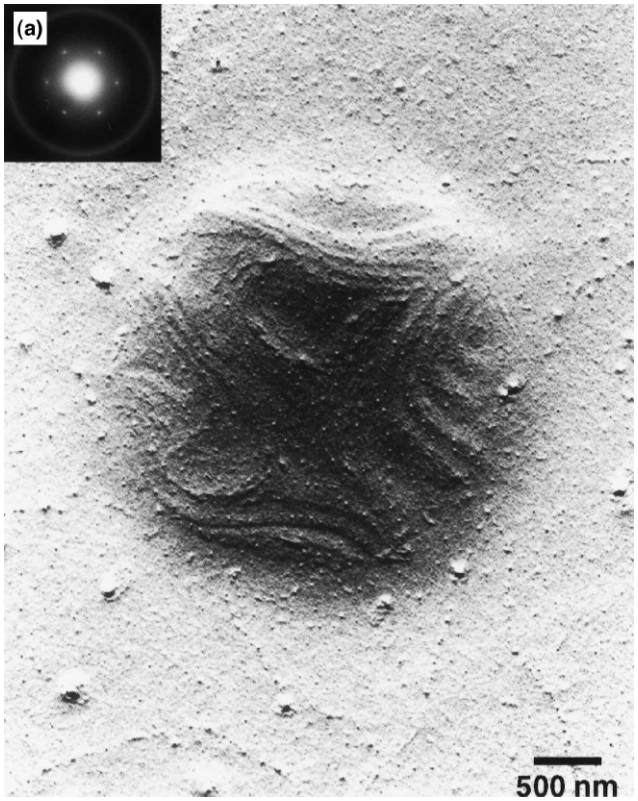

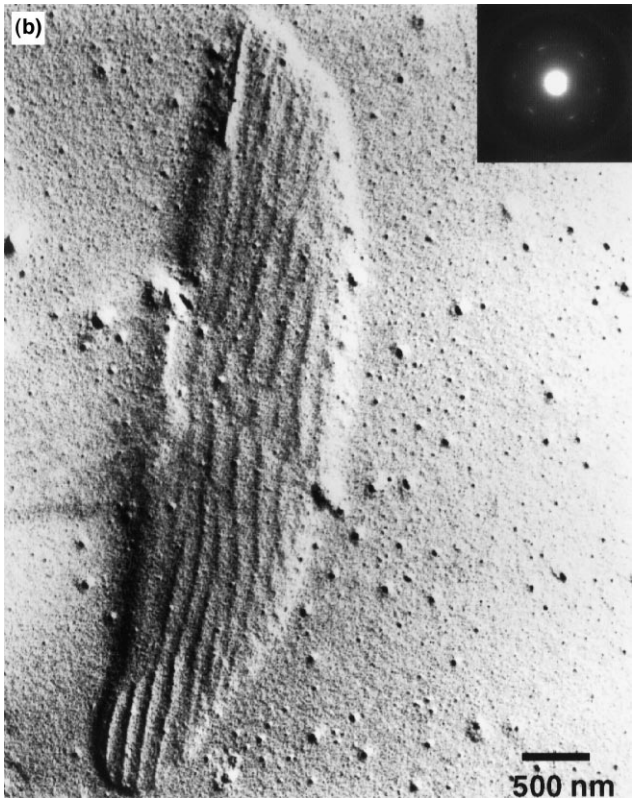

Figure 22 Monodomain morphologies and ED patterns of TPP($n = 7$) with (a) a hexagonal lateral packing and (b) an orthorhombic lateral packing[131]

being metastable in itself, but through interrupting other phase transformations, in the present example L–L phase separation. For illustrative purposes, we restrict ourselves to the L–L phase separation of a bicomponent polymer–solvent system displaying an upper critical transition (UCT).

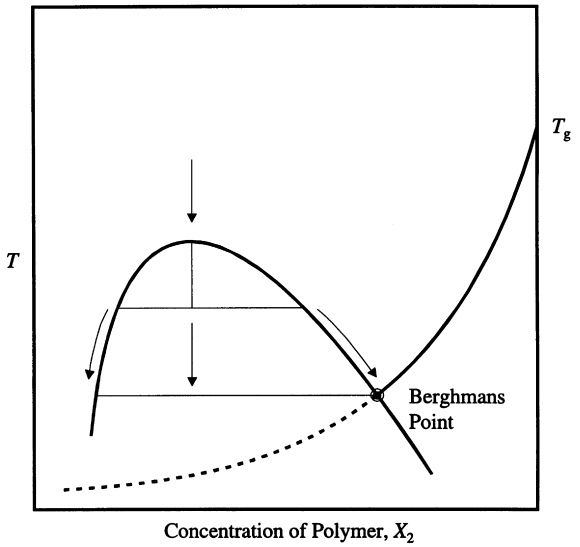

Figure 23 UCT type of liquid–liquid phase separation phase diagram with the addition of vitrification (T_g)[132]

A typical UCT phase diagram is shown schematically in *Figure 23*[132]. Upon decreasing T, we reach the UCT point, defined by a critical T (T_{cr}) and concentration (C_c). Here, we shall pay no attention to the various fundamentally important features concerning behaviour in the region of the critical point already indicated, but rather pass on to the situation arising as we further decrease T. As the two-fluid separation sets in, the system divides into two distinct phases with concentrations defined by the end points of 'tie lines' based on the 'lever rule' corresponding to each chosen T. One phase is more dilute in solute (i.e. dissolved polymer), the other in solvent, with the concentrations becoming increasingly more disparate as we move to lower Ts. In this case, just as with the vapour–liquid system of *Figure 2*, we can define within the phase line (the 'binodal' representing the condition of coexistence between the two phases) a spinodal line which is the ultimate thermodynamic limit of the stability for the homogeneous solution. The region between the two lines is the site of potential metastability where phase separation has to proceed by passing through a nucleation barrier. At the spinodal line, however, spontaneous barrier-free density fluctuation waves take over the generation of phase separation.

The morphology of the phase separation corresponding to the ultimate stability should be, as indicated previously, a two-layered liquid no matter which phase separation mechanism occurs. However, the morphologies arising on the way towards ultimate stability are basically different according to whether the phase separation is via the nucleation or spinodal mechanism: droplets for the former and a kind of bicontinuous network for the latter. There is an abundance of morphological variants even within each of the two classes, which depend on how far the still disperse but already compositionally phase segregated system has 'ripened' at the stage of inspection. Concentration is clearly a prime determining factor of the phase morphology, first because it determines whether we are in the nucleated or in the spinodal region, and secondly, within each given region it will crucially affect the sizes, shapes and mutual arrangement of the phases in their transient stage of the segregation into two layers. The latter is most easily seen in the case of the nucleation process: for systems with a low concentration of solute (polymer), the solute-rich phase will

be in the form of droplets suspended within a continuous solvent-rich matrix while there will be a matrix inversion for systems possessing a high concentration of solute and a bicontinuous geometry in systems between these two extremes.

At this point, we need to recall that in this approximation we are dealing with two distinct processes: the establishment of an equilibrium partition between the two liquids within the two phases and the evolution of the phase morphology. The first is defined by the phase diagram as in *Figure 23*, and hence, by thermodynamics, and the second by the kinetics of the process. Clearly these two processes cannot be independent of each other. This leads to issues which, to our knowledge, have not been fully addressed and hence we are not in a position to discuss. Nevertheless, it is usually true that partitioning is completed early on while the morphology is still in a stage of evolution. This means that compositionally we are already in equilibrium, while morphologically the system is still in a metastable state and can be said to be in the process of 'ripening'. As we will discuss below, even equilibrium partitioning can be thwarted through the influence of vitrification. This may create a further class of multiple metastability, i.e. a morphological, and what we may term '*compositional*', metastability. Both, while highly distinct, fall within the category of circumstantial metastability.

In a single component fluid system, vitrification occurs at the T_g. In a fully miscible bicomponent system, such as a polymer and solvent, the T_g of the polymer becomes depressed on addition of the solvent (diluent) following the T_g line in *Figure 23*. As seen, this T_g *versus* concentration line intersects the binodal at a point BP (Berghmans' Point, named after Berghmans, whose works have brought this issue to the forefront[133]). As previously described, if we cool the system below the critical point, two-fluid separation will progressively proceed as defined by the tie lines at each *T*. However, when the tie line defining BP is reached, the polymer-rich phase (and only this phase) vitrifies. This has several important consequences which we shall proceed to describe.

First, the phase morphology prevailing at the stage of vitrification will become preserved, representing a morphologically metastable state. The nature of the morphology will depend on the cooling rate and the initial concentration of the solution (the latter of course within the span of the tie line). These parameters will determine which is the disperse and which is the matrix phase, and second, whether we are in the nucleated or spinodal region. A full range of morphologies can be experimentally observed and systematically produced[134–136]. As a second important consequence, at and below the corresponding to BP not only the morphological development is arrested but all further compositional change ceases. The most direct experimental evidence of the latter is the observation that along the BP tie line the T_g becomes invariant with concentration, as first demonstrated in Berghmans' laboratory[133]. *Figure 24* shows this effect as obtained from anionically polymerized atactic polystyrene (a-PS), which is virtually monodisperse. This has allowed certain further conclusions to be reached (see below). The invariance of the T_g is a consequence of the fact that it is not only the morphology which becomes 'locked in' when going below BP (in terms of *T*), but also all further compositional change. For this reason, the above indicated compositional metastability sets in. This last issue has been addressed theoretically in both a diagrammatic form[137] and experimentally through the demonstration of 'compositional ageing' effects[136,138]. However, both are only rather cursory overviews. Further in-depth study on this important subject is clearly invited, especially to exploit the newly opened opportunity of having gained access to the intermediate stages of phase segregation in terms of composition along a given tie line through the agency of vitrification.

Connectivity is one feature of two-fluid segregated morphologies where one of the phases (the one which possesses a higher polymer concentration) deserves a separate discussion. If the vitrified phase becomes connected throughout the macroscopic sample volume, the solution converts into a gel. In fact, it is through the topic of physical gelation that the entire subject area which makes up this section has come into recent prominence, specifically, through the observation that a solution of a-PS can set as a gel upon cooling[133,134](*Figure 24*). Originally the connectivity required for gelation was considered as being provided by chain molecules which need to be long enough to become incorporated into more than one vitrified polymer rich particle (spherical latex). The long solvated chain portions form 'rubbery' bridges between these particles. Through experiments with closely monodisperse a-PS, the molecular weight requirement for establishing connectivity (hence to form a gel) could be established and was found to follow the anticipated scaling relation[135,136]. Such gels have a 'wobbly' consistency in keeping with the usual concept of a gel. However, in addition to such solvated chain connectivity, overall connectivity can also establish itself through the continuity of the glassy phase. In this case the 'gel' (retaining the term for such a system) will be stiff, robust, and glass-like, as in the rather self-evident case where phase continuity arises through the high concentration of polymer (the case of matrix inversion). The gel will also be fragile in the case where the phase continuity arises through spinodal decomposition, particularly at low concentrations where the morphology is a fine, continuous glassy lacework. In fact, under such conditions gelation can serve to identify the spinodal line in the phase diagram[131,132,136]. Specifically, the two kinds of gel, 'wobbly' and 'stiff', could be distinguished through their dramatic differences in mechanical properties which, when followed as a function of concentration at a particular *T*, can in itself serve to delineate the spinodal line[135,138] (which otherwise could also be derived theoretically[136]).

Just like all the morphologies described here, those leading to connectivity, and therefore gels, correspond to metastable states. In fact, all physical gels formed by chemically uniform homopolymers and arising through a phase transition, whether crystallization or two-fluid separation, are necessarily in a metastable state where some agency must act to arrest the phase transformation from going to completion. More precisely, these gels are at a stage of bicontinuous connectivity. In the present and conceptually simplest case, this is vitrification.

HIERARCHY OF METASTABILITIES: AN EXAMPLE IN GELATION AND CRYSTALLIZATION

The possibility of hierarchies of metastability in polymers has already been mentioned before, and has been practically featured in some of the previous discussion. In the present section we shall cite some specific cases of this hierarchy. In continuity with the preceding section on the influence of vitrification, these will be taken from the

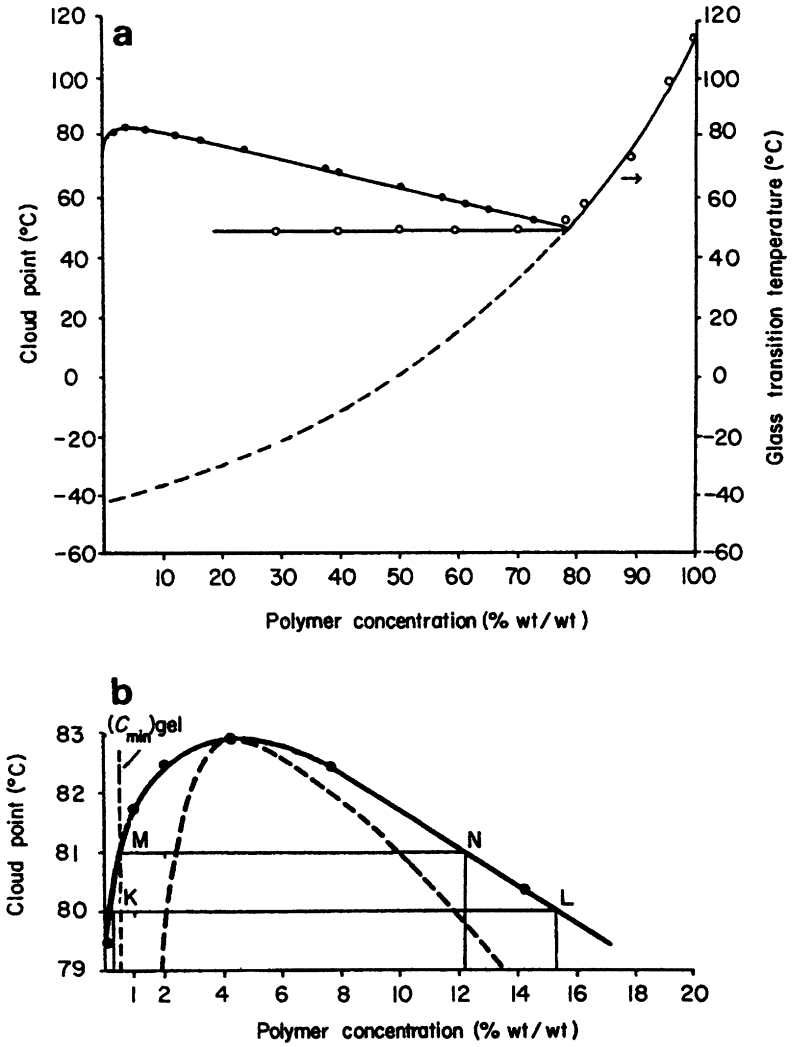

Figure 24 (a) Phase diagram of the a-polystyrene ($M_w = 2.75 \times 10^6$)/cyclohexanol system depicted in relation to the glass transition curve (the broken line is a theoretical extrapolation). (b) Enlarged detail of (a) about the commensurate point (including the spinoidal line -dashed-)[133,134]

area of two component systems, specifically polymer solutions (all corresponding to classical metastability and in the sense of traditional thermodynamics), without taking note of the influence of size and external constraints.

When the polymer–solvent systems in question are capable of crystallizing, it is this crystalline state in the appropriate crystal structure, which is the state of ultimate stability at the appropriately lowered temperature (disregarding, for the present purpose, the different levels of stability within a given crystalline system such as the chain-folded state with different fold lengths, etc.). Metastable states arise because of the high ΔTs that are often required for this crystal formation to take place at practicable rates. In the course of this ΔT change stability regime of other metastable states (by definition) may be reached. In view of previously given considerations (see e.g. *Figure 4*), once formed, these metastable phases will evolve faster than the ultimate stable phase and hence will dominate the phase transition.

The hierarchy of metastabilities arises due to the possibility of several different metastable states lying successively 'buried' beneath the state of ultimate stability in the phase diagram. These successive states can be different structures within the crystal phase category. In the following cases, they are not simply polymorphs which differ merely in terms of unit cells and atomic positions, but rather they represent distinct states which have basic influence on material behaviour. Furthermore, instead of or in addition to such polymorphs, metastability can also correspond to two-fluid separation. Finally, any or all of the corresponding phase transitions can be intercepted by vitrification. In what follows we shall discuss the situation of a 'buried' L–L phase separation to be followed by one where another crystal phase intervenes between the most stable crystal and the L–L phase lines.

In view of the complexity of real situations, some features of metastable L–L phase separation are peripheral for our purposes, we shall resort to a schematization of these concepts with reference to an actual case provided[139]. *Figure 25* schematically represents a liquid–crystal (L–C) phase diagram. The upper line corresponds to the stable L–C phase line beneath which lies a deeply 'buried' L–L phase line of UCT character. For crystallization to occur, high ΔTs are required. It is therefore possible that the L–L phase line which is 'buried' beneath the L–C line can be reached before a liquid to crystal transformation can take place. This figure shows such a situation for two ΔT values. For the smaller ΔT, ΔT_1, crystallization is expected to take place from the initial, completely mixed solution, provided sufficient time is allowed for this process. However, at the larger ΔT, ΔT_2, two-fluid separation will occur first.

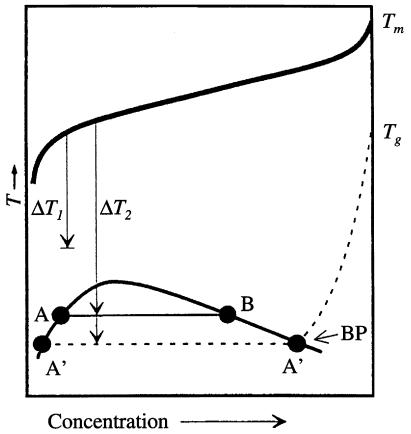

Figure 25 Schematic L–C phase diagram for a fully miscible polymer solution, also displaying metastable two-fluid separation (combined with vitrification) beneath the stable liquid–solid phase line. Depending on ΔT (or cooling rate), crystallization in the range of ΔT_1, or effects associated with two-fluid separation in the range of ΔT_2, will take place. Such situations have recently been realized with poly(phenylene ether) in cyclohexanol[139]

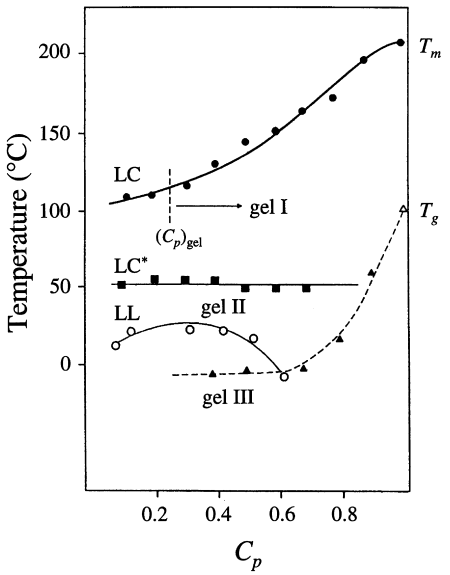

Figure 26 Phase diagram of i–PS in *trans*-decalin as an example of a system displaying a further metastable phase (L–C* phase line) intervening between the stable L–C and the metastable L–L phase lines. Each of these can give rise to gels: the liquid to crystal transition (gel I) when beyond a certain concentration $(c_p)_{gel}$; the liquid to liquid transition, combination with T_g (gel III); and the liquid to a new crystal (C*) transition, profusely gel-forming (gel II) with characteristics of its own[132,141]

Depending on how high we go in ΔT, we can have either a situation where crystallization is occurring within the concentrated phase (at B in *Figure 25*), or a situation where the concentrated phase vitrifies (as at the BP in *Figure 23*). In the latter case, not only will the L–L separation process become arrested, but also crystallization will be prevented.

We can also consider the second crystallization mode of alternative metastable crystal forms between the stable L–C and metastable L–L phase lines. A whole range of polymer–solvent systems displaying such effects with varying degrees of complexity is dealt with in a separate article by Berghmans in this same issue[140]. For now we shall look at the system of isotactic polystyrene (i-PS) in *trans*-decalin[141]. Historically, this system was the first to display the basic features of the above referred second mode crystallization and in its simplest form[142].

In the phase diagram shown in *Figure 26*, the uppermost phase line corresponds to the formation of chain folded single crystals with the macromolecules in the long-established 3_1 helical structure[143]. Such stable crystals (ignoring for the present that the chain-folded state is in itself circumstantially metastable) precipitate on cooling giving rise to a turbid suspension. If crystals form in sufficient concentration, the system can become a molecularly connected gel (gel 1 in *Figure 26*). However, when cooling is not sufficiently slow, the L–C* phase line is reached before the above mentioned crystallization has had a chance to take place (where C* represents a new crystal form). Then, at or somewhat below the L–C* line, a conspicuous new observation is evident: the whole system sets as a transparent gel very rapidly even at low concentrations. It is for this reason that this subject has come to the forefront in connection with gelation studies. For our present purposes, however, gelation is not the main point of emphasis, it merely serves as a simple indicator of a phase change having taken place far below the usual L–C phase line.

The nature of the above metastable state is still not fully resolved and is still subject of some arguments (see reference[132]). It has the character of a crystal phase prone to create connectivity, and hence is a source of gelation (gel II in *Figure 26*). The crystalline nature is apparent from WAXD whenever such patterns are obtainable. These patterns indicate a highly extended chain conformation which may be identified as a 12_1 helix[144]. The resulting morphology corresponds to a fibrilliar structure[145]. We infer that here the chains do not fold but are more or less extended. As a consequence of this their association upon crystallization is essentially interchain in nature. Therefore, this morphology favours the observed proclivity to form gels. The horizontal character of the L–C* in *Figure 26* suggests some kind of complexing with the solvent[145]. This seems to be a common feature of such a class of phenomena and it also appears in similar other systems (see reference[140]). The stoichiometry of the crystal–solvate is not yet established and such complexing does not seem to be associated with a specific solvent since the basic features of this effect are displayed by a range of different solvents. Such crystal–solvate formation is a newly emerging subject which is important in itself, however, we do not give it further emphasis in the present survey on metastability.

Passing on to lower temperatures in *Figure 26*, we reach the L–L separation line. This is manifest through turbidity appearing in the initially transparent system. In contrast to the turbidity due to the 3_1 helix containing crystals which appear beneath the LC line (after sufficiently long waiting time), the appearance of this turbidity is instantaneous and reversible with temperature. Such features comply with those of a L–L phase separation. Since the L–C* phase line cannot be traversed without at least some degree of transformation occurring, the L–L phase separation is taking place within an already partially gelified system, i.e. the chains or portions of chains which have not yet taken part in the formation of the gel junctions (those corresponding to gel II in *Figure 26*) are involved in the L–L phase separation at the correspondingly lower temperature. This picture is likely to be correct since it can be seen in experiments where the system is held for successively longer times in the temperature interval

between the L–C* and L–L lines. While the strength of the L–L phase separation on subsequent cooling, as assessed by DSC, was found to decrease progressively[132,141], the L–C* process consumed greater amounts of the material with increasing holding time. This left less and less polymer for the L–L phase separation on subsequent cooling.

On further cooling below the L–L line, the intersection with the T_g line is eventually reached as revealed by the invariance of T_g (as assessed by DSC). Here we almost return to the situation on the intervention of vitrification. The difference from the previously discussed situation is that in the present case the entire vitrifying system is in a metastable state which is deeply 'buried' beneath both the L–C and L–C* phase lines. Also, the intersection of the binodal with the T_g line should lead to a gel, but this gel will now be within a gel which had formed already when traversing the L–C* phase line. It is, therefore, not expected to be apparent as gel formation itself but merely as a stiffening of the gel which is already present to begin with. So far this phenomenon received a qualitative description, but quantification is still required.

Regarding the subject of gelation, *Figure 26* contains information on three different sources of gel formation, either simultaneously or separately, in the same system. In this figure, the turbid gel I corresponds to the formation of molecular connectivity between suspended chain-folded single crystals consisting of 3_1 helices formed from solutions of sufficiently high concentration, $(c_p)_{gel}$, beneath the L–C phase line. The transparent gel II arises through the intrinsic gel-forming ability of extended chain type of fibrous crystals consisting possibly of 12_1 helices beneath the LC* phase line, and is the most prominent of the three gelation processes. The third type of gel, gel III, is due to the interception of L–L phase separation by vitrification in the presence of sufficient phase connectivity, the effect which has been discussed separately in the previous section.

The complexity and richness in phase behaviour arising from the range of possible metastabilities, even as confined to the category of classical metastability, is apparent from the preceding discussions. It seems that, regarding systems such as that represented in *Figure 26*, we are still in the mapping process, only the first step towards reaching a comprehensive understanding. There are an increasing number of indicators that, at sufficiently high degrees of ΔT and yet still at or above the L–C* line, the conformation of the random coil itself is undergoing a transformation (most likely into a helix), and while still in isolation possibly before the onset of crystallization into the new crystal form represented by the L–C* phase line. Such changes have been indicated in i-PS[141], conclusively identified spectroscopically in i-PMMA[146] and inferred in s-PS system[147]. This would mean that at sufficient ΔT, the helix (most likely stabilized by association with solvent) is stable with respect to the random coil, where both helix and coil are metastable with respect to the ultimately stable crystal represented by the L–C phase line. Accordingly, it would be these newly formed helices which would produce gel (type gel II) by association when traversing the L–C* phase line. Thus we would have a case where the two ingredients of crystallization, adoption of a regular chain conformation and the fitting of these chains into a lattice, would occur consecutively, opposed to simultaneously as is normally envisaged. Full confirmation of this concept is still needed. The remaining uncertainties at the moment lie in the problem of making sure that helix formation actually precedes association (i.e. the gel state). This is still problematic due to the fact that once the helix has formed, association occurs very quickly. Even so, the above possibility is likely and, if real, of such potential importance that it deserves to be discussed at this stage.

Finally, a comment on the relative rates of gel formation and crystallization should be made. As already stated, crystallization upon traversing the L–C phase line is very slow. This is the general reason why the various buried metastable states can be attained. However, there is more to it than merely the sufficiently fast cooling rate outpacing the increasing acceleration of the crystallization rate with increasing ΔT. It is found that the actual rate of the stable 3_1 helix crystal formation does not keep on accelerating within the full T range between the L–C an L–C* lines, but rather, after passing through a maximum, the rate goes to a minimum which reaches negligible values before the L–C* process takes off. Therefore, it seems that both processes hamper each other in the T range where their ranges of stability start overlapping. Such a possibility was mentioned in connection with region II in *Figure 4* and has previously been supported by the observation of a pronounced minimum in crystallization rates in the case of oligomers (*n*-alkanes and PEO) at the transition region between once-folded and extended chain crystallization. We now see the same effect, i.e. a rate minimum in the *overall* transformation process, in the discussed polymer–solvent system, underpinning both the reality and generality of the underlying considerations.

CONCLUSION

In summary, we would like to emphasize that although our understanding in this field is still limited, the concepts and principles of metastable states and metastability are important aspects in polymer phase behaviour. In addition to classical metastability, we believe that circumstantial metastability, including morphological, compositional and other types of metastability, are important, specifically in polymers. These types of metastability are based on the phase size and other kinetic factors. Several issues require further consideration: first, we need to understand both the thermodynamic and kinetic limits of circumstantial metastability in polymer systems in which the classical, sharp conceptual boundary between thermodynamics and kinetics may not apply. This requires fundamental theoretical development. Second, both Monte Carlo simulations and molecular dynamics may be helpful in providing computational evidence to connecting microscopic processes with different types of metastability. Third, we must quantitatively describe the metastable states and metastability in polymer systems based on macroscopic experiments. This is perhaps not too difficult in determinations of crystal sizes and structures, but may be more complicated in other systems such as gels. Furthermore, it will be increasingly hard to study systems which approach single molecular sizes by using conventional experimental methods. Novel developments in this aspect are necessary. This list is by no means complete, but rather contains only a few selected issues. Even so, hopefully they should provide a common background to illustrate polymer phase behaviour comprising the metastable state and metastability while also raising conceptual issues regarding the meaning and definition of metastability so far, to our knowledge, unaddressed.

ACKNOWLEDGEMENTS

This work was supported by the National Science Foundation (NSF) (DMR-9157748 and 9617030), the NSF Science and Technology Center for Advanced Liquid Crystalline Optical Materials (ALCOM) at Kent State University, The University of Akron and Case Western Reserve University, the NSF/EPIC/Industry Center for Molecular and Microstructure Composites (CMMC) at Case Western Reserve University and The University of Akron, the Federal Aviation Administration, the National Aeronautics Space Administration, and the Ohio State Board of Regents. Industrial research support was provided by Phillips Petroleum, Dupont, Exxon, Hercules, Rockwell International, BP America, 3M, and others. It is most important to recognize that without the outstanding and hard research work carried out by former and current students, postdoctoral fellows, visiting scientists and visiting professors as well as the effective collaboration with colleagues at The University of Akron and other universities and institutions, and in particular, the extensive discussion and correction received from Professor P. Gujrati and Dr M. K. Chhajer, this review would never have been possible.

REFERENCES

1. Chaikin, P. M. and Lubersky, T. C., *Principles of Condensed Matter Physics*. Cambridge University Press, New York, 1995.
2. Ehrenfest, P. *Proc. Acad. Sci., Amsterdam*, Vol. 36, Sppl. 75b, Mitt. Kammerlingh Onnes Inst., Leiden, 1933, p. 153.
3. Landau, L. D., *Phys. Z. Sowejetunion*, Vol. 11, 1937, p. 26; reprinted in *Collected Papers of L. D. Lanau*, ed. D. ter Haar. Pergamon, New York, 1965.
4. Skripov, V. P., *Metastable Liquids*. John Wiley and Sons, New York, 1974.
5. Debenedetti, P. G., *Metastable Liquids, Concepts and Principles*. Princeton University Press, New Jersey, 1996.
6. Ostwald, W. Z., *Phys. Chem.*, 1897, **22**, 286.
7. Gutzow, I. and Toschew, S., *Kristall und Technik*, 1968, **3**, 485.
8. Keller, A., Hikosaka, M., Rastogi, S., Toda, A., Barham, P. J. and Goldback-Wood, G., *J. Mater. Sci.*, 1994, **29**, 2579.
9. Poon, W. C. K., Pusey, P. N. and Lakkerkerker, H., *Physics World*, April, p. 27, 1996.
10. Poon, W. C. K., Price, A. D. and Pusey, P. N., *Faraday Discuss.*, 1995, **101**, 65.
11. Evans, R. M. L., Poon, W. C. K. and Cates, M. E., *Europhys. Lett.*, 1997, **38**, 595.
12. Evans, R. M. L. and Cates, M. E., *Phys. Rev*., 1997, in press.
13. Evans, R. M. L. and Poon, W. C. K., *Phys. Rev. E*, 1997, in press.
14. Duilneveldt, Ph.D. Dissertation, Department of Chemistry, University of Utrecht, The Netherlands, 1994.
15. Ten Wolde, P. R., Ruiz Montera, M. J. and Frenkel, D., *J. Chem. Phys.*, 1996, **104**, 9932.
16. Oxtoby, D. W. and Shen, Yu Chen, *J. Phys. Cond. Matt.*, 1996, **8**, 9657.
17. Bates, F. S. and Fredrickson, G. H., *Ann. Rev. Phys. Chem.*, 1990, **41**, 525.
18. Thomas, E. L. and Lescanec, R. L., in *Self-Order and Form in Polymeric Materials*, ed. A. Keller, M. Warner and A. H. Windle. Chapman and Hall, New York, 1995, pp. 148–164.
19. Keller, A. and Goldbeck-Wood, G., in *Comprehensive Polymer Science, Supplemental Two*, ed. A. Aggewal, and Sir J. Allen. Pergamon, Oxford, 1996, pp. 241–305.
20. Geil, P., *Polymer Single Crystals*. Wiley Interscience, New York, 1963.
21. Keller, A., *Polymer Crystals, Rep. Progr. Phys.*, 1968, **31**(2), 623.
22. Wunderlich, B., *Macromolecular Physics, Crystal Structure, Morphology, Defects*, Vol. I. Academic Press, New York, 1973.
23. Bassett, D. C., *Principles of Polymer Morphology*. Cambridge University Press, New York, 1981.
24. Wunderlich, B., *Macromolecular Physics, Crystal Melting*, Vol. III. Academic Press, New York, 1980.
25. Hoffman, J. D. and Weeks, J. J., *J. Res. Natl. Bur. Stand. (Part A),*, 1962, **66**, 13.
26. Keller, A., Hikosaka, M. and Rastogi, S., *Physica Scripta*, 1996, **T66**, 243.
27. Defay, R., Prigagine, I., Belmans, A. and Everett, D. H., *Surface Tension and Adsorption*. Longmans, London, 1996.
28. Evans, R. M. L., *J. Phys. Cond. Matt.*, 1990, **2**, 8989.
29. Fischer, H. and Poser, S., *Acta Polymer*, 1996, **47**, 413.
30. Kojima, Y., Usuki, A., Kawasumi, M., Okada, A., Kurauchi, T., Kamigaito, O. and Kaji, K., *J. Polym. Sci. Polym. Phys. Ed.*, 1994, **32**, 625.
31. Hikosaka, M., Rastogi, S., Keller, A. and Kawabata, H., *J. Macromol. Sci Phys.*, 1992, **B31**, 87.
32. Bassett, D. C., Black, S. and Pierrmarini, G., *J. Appl. Phys.*, 1974, **45**, 4146.
33. Bassett, D. C. and Turner, B., *Phil. Mag.*, 1974, **29**, 925.
34. Wunderlich, B. and Melillo, L., *Makrol Chem.*, 1968, **118**, 250.
35. Rastogi, S., Hikosaka, M., Kawabata, H. and Keller, A., *Macromolecules*, 1991, **24**, 6384.
36. Hikosaka, M., Okada, H., Toda, A., Rastogi, S. and Keller, A., *J. Chem. Soc., Faraday Trans.*, 1995, **31**, 2573.
37. Rastogi, S., Unpublished results.
38. Hikosaka, M., *Polymer*, 1990, **31**, 458.
39. Arlie, J. P., Spegt, P. A. and Skoulios, A. E., *Makromol. Chem.*, 1966, **99**, 170.
40. Arlie, J. P., Spegt, P. A. and Skoulios, A. E., *Makromol. Chem.*, 1967, **104**, 212.
41. Spegt, P. A., *Makromol. Chem.*, 1970, **139**, 139.
42. Kovacs, A. J. and Gonthier, A., *Colloid and Polym. Sci.*, 1972, **250**, 530.
43. Kovacs, A. J., Gonthier, A. and Straupe, C., *J. Polym. Sci. Polym. Symp.*, 1975, **50**, 283.
44. Kovacs, A. J., Straupe, C. and Gonthier, A., *J. Polym. Sci. Polym. Symp.*, 1977, **59**, 31.
45. Kovacs, A. J. and Straupe, C., *J. Crystal Growth*, 1980, **48**, 210.
46. Kovacs, A. J. and Straupe, C., *Faraday Discuss. Chem. Soc.*, 1979, **68**, 225.
47. Buckley, C. P. and Kovacs, A., *Progr. Colloid Polym. Sci.*, 1975, **58**, 44.
48. Buckley, C. P. and Kovacs, A., *Kolloid Z. Z. Polym.*, 1976, **254**, 695.
49. Ungar, G., Stejny, J., Kellar, A., Bidd, I. and Whiting, M. C., *Science*, 1985, **229**, 386.
50. Cheng, S. Z. D., Zhang, A.-Q. and Chen, J.-H., *J. Polym. Sci. Polym. Let. Ed.*, 1990, **28**, 233.
51. Cheng, S. Z. D., Zhang, A.-Q., Chen, J.-H. and Heberer, D. P., *J. Polym. Sci. Polym. Phys. Ed.*, 1991, **29**, 287.
52. Cheng, S. Z. D., Chen, J.-H., Zhang, A.-Q. and Heberer, D. P., *J. Polym. Sci. Polym. Phys. Ed.*, 1991, **29**, 299.
53. Cheng, S. Z. D. and Chen, J.-H., *J. Polym. Sci. Polym. Phys. Ed.*, 1991, **29**, 311.
54. Cheng, S. Z. D., Zhang, A.-Q., Barley, J. S., Chen, J.-H., Habenschuss, A. and Zschack, P. R., *Macromolecules*, 1991, **24**, 3937.
55. Cheng, S. Z. D., Chen, J.-H., Zhang, A.-Q., Barley, J. S., Habenschuss, A. and Zschack, P. R., *Polymer*, 1992, **33**, 1140.
56. Cheng, S. Z. D., Chen, J.-H., Barley, J. S., Zhang, A.-Q., Habenschuss, A. and Zschack, P. R., *Macromolecules*, 1992, **25**, 1453.
57. Cheng, S. Z. D., Wu, S. S., Chen, J.-H., Zhuo, Q., Quirk, R.

P., von Meerwall, E. D., Hsiao, B. S., Habenschuss, A. and Zschack, P. R., *Macromolecules*, 1993, **26**, 5105.
58. Song, K. and Krimm, S., *J. Polym. Sci. Polym. Phys. Ed.*, 1990, **28**, 35–51.
59. Song, K. and Krimm, S., *Macromolecules*, 1989, **22**, 1504.
60. Song, K. and Krimm, S., *Macromolecules*, 1946, **1990**, 23.
61. Kim, I. and Krimm, S., *Macromolecules*, 1996, **29**, 7186.
62. Ungar, G. and Keller, A., *Polymer*, 1986, **27**, 1835.
63. Ungar, G. and Keller, A., *Polymer*, 1899, **1987**, 28.
64. Lauritzen, J. I. Jr. and Hoffman, J. D., *J. Appl. Phys.*, 1973, **44**, 4340.
65. Hoffman, J. D., Frolen, L. J., Ross, G. S. and Lauritzen, J. I. Jr., *J. Res. Natl. Bur. Stand. Sect. A*, 1976, **71A**, 261.
66. Hoffman, J. D., Davis, G. T., Lauritzen, J. I. Jr. in *Treatise on Solid State Chemistry*, Vol. 3, Chapter 7, ed. N. B. Hannay. Plenum, New York, 1976, pp. 497-614.
67. Hoffman, J. D., *Polymer*, 1982, **23**, 656.
68. Hoffman, J. D., *Polymer*, 1983, **24**, 3.
69. Hoffman, J. D. and Miller, R. L., *Macromolecules*, 1988, **21**, 3038.
70. Hartly, A., Leung, Y. K., Booth, C. I. and Shepherd, I. W., *Polymer*, 1976, **17**, 354.
71. Fraser, M. J., Marshall, A. and Booth, C., *Polymer*, 1977, **18**, 93.
72. Ashman, P. C. and Booth, C., *Polymer*, 1973, **14**, 300.
73. Cooper, D. R. and Booth, C., *Polymer*, 1977, **18**, 164.
74. Shimada, T., Okui, N. and Kawai, T., *Makromol. Chem.*, 1980, **181**, 2643.
75. Galin, J.-C., Spegt, P. A., Suzuki, S. and Skoulios, A. E., *Makromol. Chem.*, 1974, **175**, 991.
76. Thierry, A. and Skoulios, A. E., *Colloid and Polym. Sci.*, 1977, **255**, 334.
77. Thierry, A. and Skoulios, A. E., *Eurp. Polym. J.*, 1977, **13**, 169.
78. Lee, S.-W., Chen, E., Zhang, A.-Q., Moon, B., Lee, S., Harris, F. W., Cheng, S. Z. D., von Meerwall, E. D., Hsiao, B. S., Verma, R. and Lando, J., *Macromolecules*, 1996, **29**, 8816.
79. Morgan, R. L., Hill, M. J., Barham, P. J., Keller, A. and Organ, S. J., *J. Polym. Sci. Polym. Phys. Ed.*, in press.
80. Natta, G., Pasquon, I., Corradini, P., Peraldo, M., Pegoraro, M. and Zambelli, A., *Rend. Acc. Naz. Lincei*, 1960, **28**, 541.
81. Lotz, B., Lovinger, A. J. and Cais, R. E., *Macromolecules*, 1988, **21**, 2375.
82. Lovinger, A. J., Lotz, B. and Davis, D., *Polymer*, 1990, **31**, 2253.
83. Lovinger, A. J., Davis, D. and Lotz, B., *Macromolecules*, 1991, **24**, 552.
84. Lovinger, A. J., Lotz, B., Davis, D. and Padden, F. J. Jr., *Macromolecules*, 1993, **26**, 3494.
85. De Rosa, C. and Corradini, P., *Macromolecules*, 1993, **26**, 5711.
86. Rodriguez-Arnold, J., Bu, Z. and Cheng, S. Z. D., *J. Macromol. Sci. Review of Macromol. Chem. Phys.*, 1995, **C35**, 117.
87. Bu, Z., Yoon, Y., Ho, R.-M., Zhou, W., Jangchud, I., Eby, R. K., Cheng, S. Z. D., Hsieh, E. T., Johnson, T. W., Geerts, R. G., Palackal, S. J., Hawley, G. R. and Welch, M. B., *Macromolecules*, 1996, **29**, 6575.
88. Wittmann, J.-C. and Lotz, B., *Makromol. Chem. Rapid Commun.*, 1982, **3**, 733.
89. Wittmann, J.-C. and Lotz, B., *J. Polym. Sci. Polym. Phys. Ed.*, 1985, **23**, 205.
90. Zhou, W. and Cheng, S. Z. D., Unpublished results.
91. Avakian, P., Gardner, K. H. and Matheson, R. P. Jr., *J. Polym. Sci. Polym. Symp.*, 1990, **28**, 243.
92. Blundell, D. J. and Newton, A. B., *Polymer*, 1991, **32**, 308.
93. Gardner, K. H., Hsiao, B. S., Matheson, R. P. Jr. and Wood, B. A., *Polymer*, 1992, **33**, 2484.
94. Gardner, K. H., Hsiao, B. S. and Faron, K. L., *Polymer*, 1994, **35**, 2290.
95. Ho, R.-M., Cheng, S. Z. D., Hsiao, B. S. and Gardner, K. H., *Macromolecules*, 1994, **27**, 2136.
96. Ho, R.-M., Cheng, S. Z. D., Fisher, H. P., Eby, R. K., Hsiao, B. S. and Gardner, K. H., *Macromolecules*, 1994, **27**, 5787.
97. Ho, R.-M., Cheng, S. Z. D., Hsiao, B. S. and Gardner, K. H., *Macromolecules*, 1995, **28**, 1938.
98. Cheng, S. Z. D., Ho, R.-M., Hsiao, B. S. and Gardner, K. H., *Macromol. Chem. Phys.*, 1996, **197**, 185.
99. Lehmann, O., *Uber Physikalische Isomerie (from Keller, H., 1877. History of Liquid Crystals*). *Mol. Cryst. Liq. Cryst.*, 1973, **21**, 1.
100. Percec, V. and Keller, A., *Macromolecules*, 1990, **23**, 4347.
101. Carr, N. and Gray, G. W., *Mol. Cryst. Liq. Cryst.*, 1985, **124**, 27.
102. Andrews, B. M. and Gray, G. W., *Mol. Cryst. Liq. Cryst.*, 1985, **123**, 257.
103. Ungar, G., Feijoo, J. L., Keller, A., Yourd, R. and Percec, V., *Macromolecules*, 1990, **23**, 244.
104. Cheng, S. Z. D., Yandrasits, M. A. and Percec, V., *Polymer*, 1991, **32**, 1284.
105. Yandrasits, M. A., Cheng, S. Z. D., Zhang, A.-Q., Cheng, J.-L., Wunderlich, B. and Percec, V., *Macromolecules*, 1992, **25**, 2112.
106. Heberer, D. P., Keller, A. and Percec, V., *J. Polym. Sci. Polym. Phys. Ed.*, 1995, **33**, 1877.
107. Pardey, R., Wu, S. W., Chen, J.-H., Harris, F. W., Cheng, S. Z. D., Keller, A., Aducci, J., Facinelli, J. V. and Lenz, R. W., *Macromolecules*, 1994, **27**, 5794.
108. Cheng, S. Z. D., *Macromolecules*, 1988, **21**, 2475.
109. Cheng, S. Z. D., Janimak, J. J., Lipinski, T. M., Sridhar, K., Huang, X.-Y. and Harris, F. W., *Polymer*, 1990, **31**, 1122.
110. Jonsson, H., Wallgren, E., Hult, A. and Geedde, U. W., *Macromolecules*, 1990, **23**, 1041.
111. Cheng, S. Z. D., Johnson, R. L., Wu, Z. and Wu, H. H., *Macromolecules*, 1991, **24**, 150.
112. Campoy, I., Marco, C., Gomez, M. A. and Fatou, J. G., *Macromolecules*, 1995, **25**, 4392.
113. Pardey, R., Harris, F. W., Cheng, S. Z. D., Aducci, J., Facinelli, J. V. and Lenz, R. W., *Macromolecules*, 1992, **25**, 5060.
114. Pardey, R., Harris, F. W., Cheng, S. Z. D., Aducci, J., Facinelli, J. V. and Lenz, R. W., *Macromolecules*, 1993, **26**, 3687.
115. de Gennes, P.-G., *Mol. Cryst. Liq. Cryst. Lett. Sect.*, 1984, **102**, 95.
116. Chandrasekhar, S., *Liquid Crystal*, 2nd Edn. Cambridge University Press, New York, 1992.
117. Gray, G. W. and Goodby, J. W. G., *Smectic Liquid Crystals*. Leonard Hill, London, 1984.
118. Pershan, P. S., *Structure of Liquid Crystal Phases*. World Scientific, Singapore, 1988.
119. Meurisse, P., Noel, C., Monnerie, L. and Fayolle, B., *Brit. Polym. J.*, 1981, **13**, 55.
120. Ober, C., Jin, J.-I. and Lenz, R. W., *Polymer J. (Japan)*, 1982, **14**, 9.
121. Krigbaum, W. R., Asrar, J., Toriumi, H., Ciferri, A. and Preston, J., *J. Polym. Sci. Polym. Lett.*, 1982, **20**, 109.
122. Coassolo, A., Foá, M., Dainelli, D., Scordamaglia, R., Barino, L., Chapoy, L. L., Rustichelli, F., Yang, B. and Torquati, G., *Macromolecules*, 1991, **24**, 1701.
123. Carotenuto, M. and Iannelli, P., *Macromolecules*, 1992, **25**, 4373.
124. Percec, V., Chu, P., Ungar, G., Cheng, S. Z. D. and Yoon, Y., *J. Mater Chem.*, 1994, **4**, 719.
125. Yoon, Y., Zhang, A.-Q., Ho, R.-M., Cheng, S. Z. D., Percec, V. and Chu, P., *Macromolecules*, 1996, **9**, 294.
126. Cheng, S. Z. D., Yoon, Y., Zhang, A.-Q., Savitski, E. P., Park, J.-Y., Percec, V. and Chu, P., *Macromol. Rapid Commun.*, 1995, **16**, 533.
127. Yoon, Y., Ho, R.-M., Moon, B., Kim, D., McCreight, K. W., Li, F., Harris, H. W., Cheng, S. Z. D., Percec, V. and Chu, P., *Macromolecules*, 1996, **29**, 3421.

128. Sirota, E. B., Pershan, P. S., Sorensen, L. B. and Collett, J., *Phys. Rev. A.*, 1987, **36**, 2890.
129. Tweet, D. J., Holyst, R., Swanson, B. D., Stragier, H. and Sorensen, L. B., *Phys. Rev. Lett.*, 1990, **65**, 2157.
130. Galerne, Y. and Liebert, L., *Phys. Rev. Lett.*, 1991, **66**, 2891.
131. Ho, R.-M., Yoon, Y., Leland, M., Cheng, S. Z. D., Yang, D., Percec, V. and Chu, P., *Macromolecules*, 1996, **29**, 4528.
132. Keller, A., *Faraday Discuss.*, 1995, **101**, 1.
133. Arnouts, J. and Berghmans, H., *Polymer Commun.*, 1987, **28**, 66.
134. Hikmet, R. M., Callister, S. and Keller, A., *Polymer*, 1988, **29**, 1377.
135. Callister, S., Keller, A. and Hikmet, R. M., *Makromol. Chem. Macromol. Symp.*, 1990, **39**, 19.
136. Arnauts, J., Berghmans, H. and Koningsveld, R., *Macromol. Chem.*, 1993, **194**, 77.
137. Frank, F. C. and Keller, A., *Polym. Commun.*, 1988, **29**, 186.
138. Callister, S., Ph.D. Dissertation, Department of Physics, Bristol University, 1989.
139. Berghmans, S., Mewis, J., Berghmans, H. and Meiger, H., *Polymer*, 1995, **36**, 3085.
140. Berghmans, H., De Cooman, R., De Rudder, J., Koningsveld, R., *Polymer*, to appear in this issue.
141. Ohara, T., France, C. and Keller, A., Unpublished results.
142. Girolamo, M., Keller, A., Miyasaka, K. and Overbergh, N., *J. Polym. Sci. Polym. Phys. Ed.*, 1976, **14**, 391.
143. Natta, G., Corradini, P. and Bassi, I. W., *Nuovo. Cima.*, 1960, **15**(S1), 68.
144. Atkins, E. D. T., Isaac, D. H., Keller, A. and Miyasaka, K., *J. Polym. Sci. Polym. Phys. Ed.*, 1977, **15**, 211.
145. Atkins, E. D. T., Hill, M. J., Jarvis, D. A., Keller, A., Sathene, E. and Shapire, J., *Colloid Polym. Sci.*, 1984, **262**, 22.
146. Berghmans, S., Thijs, S., Cornette, M., Berghmans, H., De Schryver, F. C., Moldenaers, P. and Mewis, J., *Macromolecules*, 1994, **27**, 7669.
147. Deberdt, F. and Berghmans, H., *Polymer*, 1993, **35**, 1694.